# SNOWMELT HYDROLOGY IN THE UPPER KUPARUK WATERSHED, ALASKA: OBSERVATIONS AND MODELING

By

Kelsey M Dean, B.S.

A Thesis Submitted in Partial Fulfillment of the Requirements

for the Degree of

Masters of Science

in

Water and Environmental Science

Concentration Area Hydrology

University of Alaska Fairbanks

August 2019

APPROVED:

Svetlana Stuefer, Committee Chair
David Verbyla, Committee Member
William Schnabel, Committee Member
Robert Perkins, Department Chair
*Department of Civil and Environmental Engineering*
William Schnabel, Dean
*College of Engineering and Mines*
Michael Castellini, *Dean of the Graduate School*

# Abstract

The Fourth National Climate Assessment Report (2018) indicates that Alaska has been warming at a rate two times greater than the global average with the Arctic continuing to be experiencing higher rates of warming. Snowmelt driven runoff is the largest hydrologic event of the year in many Alaska Arctic river systems. Changes to air temperature, permafrost, and snow cover impact the timing and magnitude of snowmelt runoff. This thesis examines the variability in hydrometeorological variables associated with snowmelt to better understand the timing and magnitude of snowmelt runoff in headwater streams of Arctic Alaska. The objectives of this thesis are to: (1) use observational data to evaluate trends in air temperature, precipitation, snow accumulation, and snowmelt runoff data; (2) relate precipitation, snow cover, and air temperature to snowmelt runoff using the physically-based Snowmelt Runoff Model (SRM) to test the applicability of the model for headwater streams in the Arctic. The focus of this study is the Upper Kuparuk watershed area, located in Alaska on the north side of the Brooks Range, where several monitoring programs have operated long enough to generate a 20-year climate record, 1993-2017. Long-term air temperature, precipitation, and streamflow data collected by the University of Alaska Fairbanks at the Water and Environmental Research Center and other agencies were used for statistical analysis and modeling.

While no statistically significant trends in snow accumulation and snowmelt runoff were identified during 1993-2017, observations highlight large year-to-year variability and include extreme years. Snow water equivalent ranges from 5.4 to 17.6 cm (average 11.0 cm), peak snowmelt runoff ranges from 3.84 to 50.0 cms (average 22.4 cms), and snowmelt peak occurrence date ranges from May 13 to June 5 for the Upper Kuparuk period of record. The spring of 2015 stands out as the warmest, snowiest year on record in the Upper Kuparuk.

To further investigate the runoff response to snowmelt in 2015, remote sensing snow data was analyzed and recommended parameters were developed for SRM use in the Upper Kuparuk watershed. Recommended parameters were then applied to 2013 snowmelt runoff as a test year. Model results varied between the two years and provide good first-order approximation of snowmelt runoff for headwater rivers in the Alaska Arctic.

# Table of Contents

# List of Figures

# List of Tables

# Acknowledgements

Financial support for this thesis was provided by the National Institute of Water Resources with additional contributions. I would like to thank all the Water and Environmental Research Center faculty and students that have collected data from the Upper Kuparuk and Imnavait watersheds throughout the years. I would like to acknowledge the support and guidance of my advisor Sveta Stuefer and committee members William Schnabel and David Verblya throughout my master's program. I would also like to thank Jaroslav Martinec and Albert Rango for creating the open source Snowmelt Runoff Model as well as the National Snow and Ice Data Center for the publicly available MODIS imagery and products.

# 1. Introduction

Watersheds in the Arctic are complex hydrologic systems sensitive to shifts in surface energy budget, decrease in sea ice extent, warming permafrost, and prolonged snow accumulation (Adam et al., 2009; Bokhorst et al., 2016: Kane et al., 2008). Arctic landscapes are dominated by snow for 8 to 10 months out of the year, with the possibility of snow any month (Benson & Sturm, 1993; Callaghan et al., 2011). The Arctic is facing the effects of climate change at an unprecedented rate. Surface air temperature has increased double the amount compared to the rest of the world and has surpassed the temperature increase predicted by climate change models (Larsen et al., 2014; Overland et al., 2018). Snow cover extent, particularly in the spring and fall, across the Arctic is decreasing and predicted to continue the decreasing trend (Callaghan et al., 2011; Liston & Hiemstra, 2011; Mudryk et al., 2018). Due to the relationship between Arctic climate and the reduction in sea ice extent, models have predicted that the amount of precipitation in the Arctic will increase due to increased local evaporation from the open coastal waters (Bintanja & Selten, 2014). This local moisture recycling is one of the factors affecting extreme runoff events observed in Arctic coastal watersheds in Alaska during the past decade (Bintanja & Selten, 2014; S. L. Stuefer et al., 2017).

Snow and permafrost driven hydrology elicits unique responses in storage capacity and spring runoff flooding (Hinzman et al., 2005; Woo, 2010). Rapid ablation of snow covered areas and limited subsurface water storage capacity in continuous permafrost regions make snow driven runoff the largest annual hydrologic event in the Arctic (Kane et al., 1997; McNamara et al., 1998). Compared to other hydrologic systems in the world, snowmelt runoff in Alaska Arctic tundra systems occurs in a short time period in May and June with snow cover melting in 7 to 14 days (Kane et al., 1997; Stuefer et al., 2014).

Forecasting the magnitude of snowmelt runoff and establishing long-term trends in snowmelt hydrology in the Alaska Arctic is limited by amount and longevity of continuous streamflow and snow cover measurements (Kane et al., 2003; Kane et al., 2008; Stuefer et al., 2017). Since the development of the Alyeska pipeline in the 1970s, emphasis on gaging and monitoring stream crossings in the Alaska Arctic has become a priority with the Alaska Department of Transportation & Public Facilities (ADOT&PF), Bureau of Land Management (BLM), and U.S. Geological Survey (USGS). Interest in Alaska Arctic hydrology has continued

since then with emphasis on resource development, land conservation, and climate monitoring. Extreme events, including snowmelt flooding, are also predicted to double in the upcoming years (IPCC, 2014). Shifts in the amount, characteristics, and timing of snowmelt driven runoff could lead to reoccurrence of extreme flooding events with negative impacts on infrastructure, economies, and communities in Alaska.

Previous hydrologic modeling in headwater watersheds in Alaska Arctic have included the application of TopoFlow, HBV, and various other models (Hinzman, 1990; Kane et al., 1997; Schramm et al., 2007). These models have begun to offered insight into the complex hydrologic systems seen in the Arctic and characterize hydrologic aspects of Alaska Arctic watersheds including the impacts of permafrost, peak flow timing, and storm events. Modeling snowmelt runoff using accessible data could provide insight and tools for land management and decisions while providing an understanding Arctic trends at a local watershed level.

The purpose of my research is to accomplish the following research objectives. The first research objective is to use observational data to evaluate trends in historical air temperature, precipitation, snow accumulation, and snowmelt runoff data. The second research objective is to relate precipitation, snow, and air temperature to snowmelt runoff using physically-based Snowmelt Runoff Model (SRM) to test the applicability of the model for headwater streams in the Arctic.

# 2. Study Area

The study area, Upper Kuparuk watershed, is in the foothills on the northern side of the Brooks Range and is the headwaters of the Kuparuk River. The site was established in 1993 by the Water and Environmental Research Center (WERC) with the installation of a stream gage and a meteorological station, one of the few basin-wide long-term monitoring systems in northern Alaska. The watershed is located adjacent to the Imnavait Creek, established in 1985, one of the longest monitored watersheds in the area. While Imnavait watershed joins the Kuparuk River downstream of the Upper Kuparuk gaging station, it shares the eastern watershed boundary and provides historical observations of snow, rainfall, and air temperature data which were used as supplemental and comparison data for this study. The number of meteorological stations in the study area have fluctuated throughout the period of record, with the UKmet station (Figure 1) having the most complete, continuous record and still in operation today. The location of the study area, meteorological stations, gaging locations, and snow survey sites are shown in Figure 1.

The Upper Kuparuk watershed is representative of medium sized foothill watershed on the north side of the Brooks Range based on landscape and terrain characteristics. The watershed is 130.5 $km^2$ and ranges from 738 m to 1519 m in elevation with a mean elevation of 986 m. The stream is frozen from late September to mid-May annually. Continuous permafrost underlies the entire area (Kane et al., 1997). Seasonal thaw depths range from 25 cm to 100 cm in the area (Kane et al., 2004). The Upper Kuparuk composes less than 1.7% of the watershed area for the Kuparuk River (McNamara et al., 1998). However, historical analysis have shown that during snowmelt the Upper Kuparuk can contribute up to 7% of the Kuparuk's snowmelt runoff demonstrating the importance of the headwater streams to downstream volumes of northern coastal rivers (McNamara et al., 1998).

The region is characterized by arctic vegetation and a limited summer growing season (Walker et al., 1989). Dwarf birch, tussocks, lichen and moss are the primary vegetation throughout the area (Walker et al., 1989). The lower portions of the watershed are composed of small shrubs and willows. Rolling foothills extend into the upper mountainous regions transition into alpine vegetation communities. There are several small lakes located in the upper portion of

the watershed that serve as overwintering habitat for arctic grayling populations (Deegan et al., 1999).

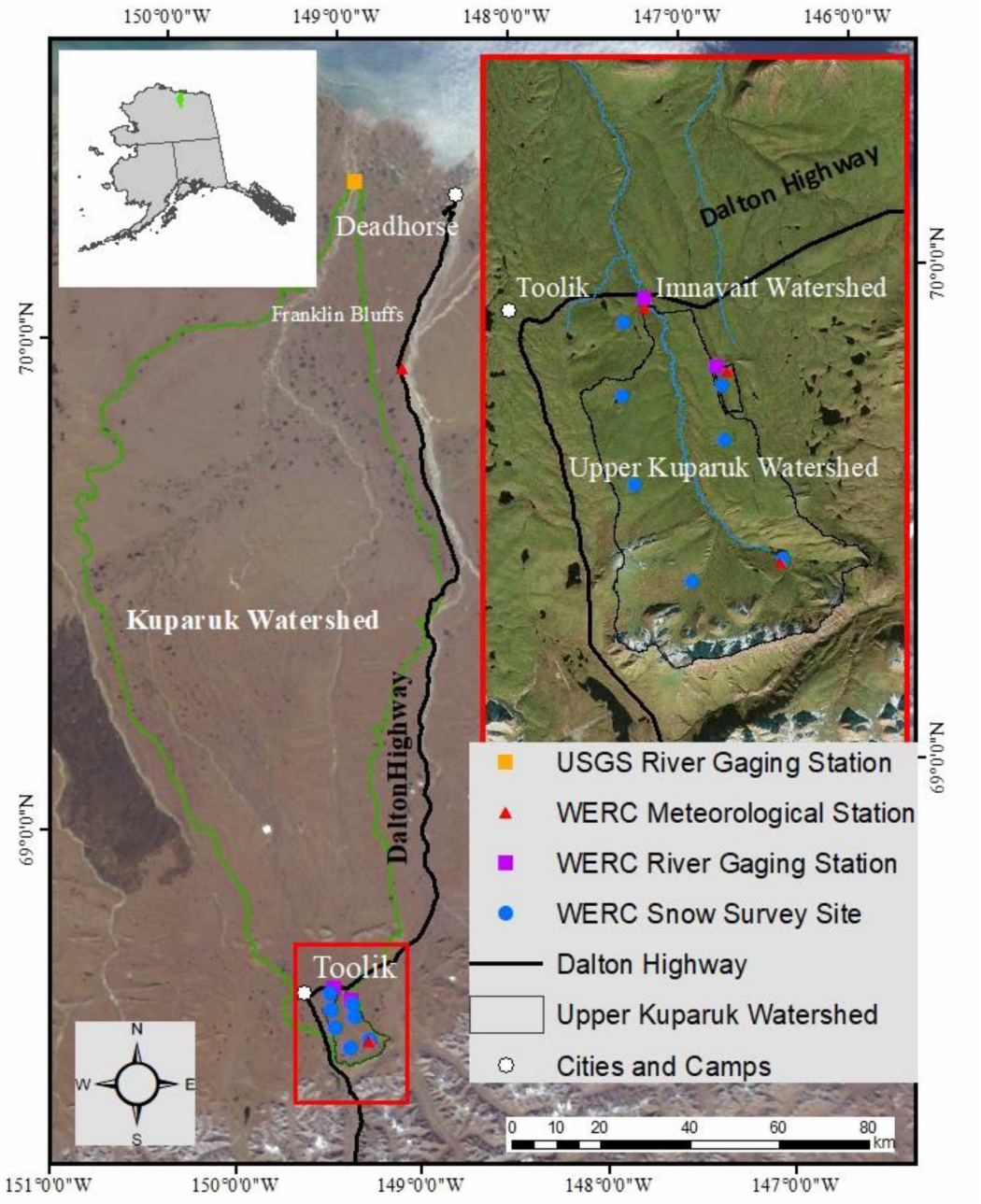


*Figure 1. Location map of the Upper Kuparuk watershed. Gaging stations, meteorological instrumentation, and snow survey locations are shown within the Upper Kuparuk area. Insert shows location of the Upper Kuparuk in the state of Alaska. The watershed boundary is shown in black.*

# 3. Data

In order to complete the research objectives long-term, spatially distributed hydrologic and meteorological data was required. This section describes hydrologic, meteorologic, and remote sensing data used.

## 3.1 Stage and Discharge

Discharge measurements from 1993-2017 are provided from a stilling well gage house and staff gage (68.642280 W, -149.40 N) collected by WERC students and faculty (Table 1). WERC uses a rating curve relating stage and discharge to produce instantaneous discharge measurements. Instantaneous stage was collected during snowmelt in the spring to the fall, mid-May to late August annually. Rating curves only function in open water conditions. During ice-affected conditions increase frictional forces on the water result in backwater making rating curve inaccurate. To provide accurate discharge estimates during ice-affected conditions, discrete field discharge measures were conducted to provide discharge estimates during snowmelt based on field measurements taken twice a day.

Automated stage measurements are transmitted to the WERC at University of Alaska Fairbanks (UAF) where post processing occurs. Discharge data for Upper Kuparuk was downloaded from *http://ine.uaf.edu/werc/werc-projects/teon/current-stations/upper-kuparuk-river.*

*Table 1. Summary of hydrometeorological data available for the Upper Kuparuk from WERC.*

| Observations | Period of Records | Missing Years |
|---|---|---|
| **Stage/Discharge** | 1993-2017 | - |
| **Air Temperature** | 1993-2017 | - |
| **Rainfall** | 1995-2017 | 2000, 2001, 2014 |
| **Snow Water Equivalent** | 1996-2017 | 2014 |

## 3.2 Meteorological

### 3.2.1 Air Temperature

UKmet station (Figure 1) air temperature from the 1993-2017 was downloaded from *http://ine.uaf.edu/werc/werc-projects/teon/current-stations/upper-kuparuk*. Hourly year-round air temperature is measured in the Upper Kuparuk from three different heights: 10 m, 3 m, and 1.5. For this study 3 m air temperature was used. The meteorological station is in a snow drift that can persist into June, distorting the 1.5 m air temperature during snowmelt. Hourly temperature measurements were converted into a daily average for analysis and model inputs.

### 3.2.2 Precipitation

Precipitation for this study is represented by two categories: rainfall and snow accumulation on the ground. WERC collects rainfall at the UKmet station (Figure 1) using an 8-inch tipping bucket with an Alter shield and computed into cumulative rainfall for the year. Cumulative rainfall was defined as the sum of all precipitation occurring after the first five-day period of air temperatures above 0°C and before the first five consecutive days of below freezing temperature in the fall, typically May to September. Cumulative rainfall from 1994-2013 was used from published data reports (Kane et al., 2014). Cumulative rainfall from 2014- 2017 was computed using the same methods. Daily rainfall data was downloaded from *http://ine.uaf.edu/werc/werc-projects/teon/current-stations/upper-kuparuk*.

The second component of precipitation, snow accumulation, is represented by seasonal maximum snow water equivalent (SWE). Due to the difficultly and errors associated with the collection of continuous snowfall measurements in the Arctic with precipitation gages, an annual SWE measurements are used to represent snow accumulation throughout the winter months. SWE in the Upper Kuparuk have been collected from 1996- 2017, excluding 2014, using repeat field measurements, sites, and methods. To compute SWE, multiple snow depth and density measurements are taken in late April to early May, the end of the snow accumulation, to calculate a basin wide SWE (Figure 1).

Historically, snowpack ablation has also been monitored throughout the melt season in the Upper Kuparuk and Imnavait Creek. However, since 2013 a single annual snow survey has been conducted and ablation is no longer monitored. The Natural Resource Conservation Service

(NRCS) snow telemetry site 968 (SNOTEL) located in the Imnavait watershed was used as substitution for ablation data when data within the Upper Kuparuk was not available and as comparison precipitation data, *https://wcc.sc.egov.usda.gov/nwcc/site?sitenum=968*.

## 3.3 Remote Sensing Data

### 3.3.1 MODSCAG

One of the primary components of the Snowmelt Runoff Model is snow covered area (SCA), see section 4.2 for further explanation. Optical remote sensing is an ideal to map SCA due to the high reflectance, albedo, of snow. There are a variety of optical remote sensing products that can be used to map SCA including Landsat, MODIS, SPOT and NOAA VHRR. However, the rapid nature of snowmelt in the Arctic makes remote sensing product such as Landsat Thematic Mapper, 16 day frequency, irrelevant for the snowmelt period (Kane et al., 2008). The MODIS snow fraction product MODSCAG (MODIS Snow Covered-Area and Grain size retrieval algorithm) was chosen for the study due to its availability as a daily product. Previous comparative product studies have shown that the MODSCAG product is accurate for use with the SRM model (Lee et al., 2005; Raleigh et al., 2013; Rittger et al., 2013; Steele et al., 2017).

MODSCAG provides a daily fractional snow-covered area for 500 m resolution pixels. MODSCAG is a regional product derived from MODIS Surface-Reflectance Product analyzing the MODIS near infrared, visible, and shortwave infrared bands (Painter et al., 2009). Each 500 m pixel is assigned either a fraction of snow cover (1-100), no data, or cloud cover qualifier. Processed TIFFS for the period and area of interest were downloaded from NASA Jet Propulsion Laboratory Snow Data System Portal (*https://snow.jpl.nasa.gov/portal/data*).

### 3.3.2 Digital Elevation Model

The Upper Kuparuk watershed boundary was delineated using 5 m resolution Digital Elevation Model (DEM) from 2002 obtained from *https://toolik.alaska.edu/gis/data/index.php* (Nolan, 2002).

## 3.4 Snowmelt Runoff Model: Model Configuration

The Snowmelt Runoff Model (SRM) is a physically based temperature-index model that uses air temperature, precipitation, and snow-covered area and eight calibration parameters to produced daily runoff for a basin (Martinec et al., 2008). The SRM was developed by Jaroslavo Martinec in the 1970s and originally applied in mountainous watersheds in Switzerland (Martinec, 1975). Further development of SRM was done in conjunction with the U.S. Forest Service and New Mexico State University, where the model is currently housed in a graphic user interface (Martinec et al., 2008). Historically, SRM was made to model exclusively snowmelt runoff, however, with version improvements year-round runoff can now be modeled. SRM can be used as a forecasting tool and to model climate change scenarios. SRM has been successfully applied across the world in over 100 basins of varying size and elevation ( Martinec et al., 2008).

SRM is run in zones, hydrologic response units, based on elevation to account for variation in SCA, air temperature, and precipitation impacting runoff. Up to 16 different zones are allowed within the SRM framework. SRM is governed by the following equation:

$$Q_{n+1} = [c_{sn} * a_n(T_n + \Delta T_n)S_n + c_{rn} * P_n]\frac{A * 10000}{84600}(1 - k_{n+1}) + Q_n * k \qquad (1)$$

Where $Q_{n+1}$ is the calculated daily discharge; $c_s$ is the snow runoff coefficient; a is the degree-day factor; T is the number of degree days; $\Delta T$ is the temperature adjustment for elevation; S is the ratio of SCA; $c_r$ is the rain runoff coefficient; P is the amount of new precipitation; is the watershed area (A) and conversion factor from cm $km^2$ $d^{-1}$ to $m^3$ $s^{-1}$; k is the recession coefficient during periods without new snowfall or rainfall; and $Q_n$ is the previous time steps runoff. The equation is used on each individual zone and summed for a total daily discharge value.

SRM uses eight parameters: temperature lapse rate, lag time, rain contributing area, runoff coefficients (snow and rain), critical temperature, degree-day factor, and recession coefficient. Parameters are based on physical and hydrologic processes of a basin. A summary of the parameters is found in Table 2.

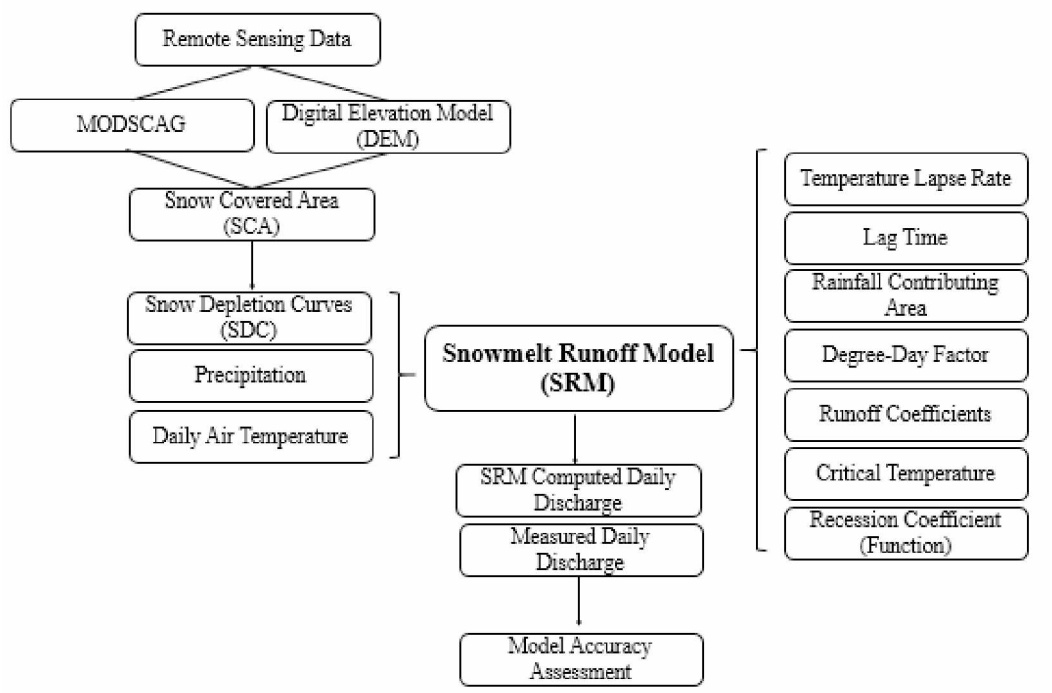


*Figure 2. Snowmelt Runoff Model structure including inputs and parameters.*

*Table 2. Snowmelt Runoff Model parameter summary (adapted from* Katwijk et al., 1993)

| Parameter | Symbol | Description |
|---|---|---|
| **Runoff Coefficient Snow** | $C_s$ | The amount of available water for runoff from snowmelt. |
| **Runoff Coefficient Rain** | $C_R$ | The amount of available water for runoff from rainfall. |
| **Degree Day Factor** | α | Coefficient (cm $d^{-1}C^{-1}$) that relates degree-days to a daily snowmelt depth (cm). |
| **Temperature Lapse Rate** | ϒ | Rate of temperature change per unit change in 100 m elevation (°C/100m). |
| **Critical Temperature** | $T_{CRIT}$ | Temperature at which precipitation occurs as snow instead of rain. |
| **Rainfall Contributing Area** | RCA | Qualifier of the ripeness of the snowpack and it determines when precipitation will move through the snowpack becoming immediately available for runoff. |
| **Recession Coefficient (Function)** | *k* | Function associated with the decline in runoff during periods with no new precipitation or snowmelt and the transfer function for the model. |
| **Lag Time** | L | Time before the melt water and precipitation appear as runoff. |

# 4. Methods

## 4.1 Hydrometeorological Variables

This study is focused on six hydrometeorological variables associated with snowmelt runoff for trend analysis and identification of model years: May positive degree days (PDD), peak and date of occurrence of snowmelt discharge, cumulative rainfall, SWE, and volume of snowmelt runoff (Table A1). Mean, standard deviation, and coefficient of variation of the hydrometeorological variables were calculated and examined for the Upper Kuparuk for the available period of record.

May positive degree days (PDD) is the sum of the mean daily air temperature greater than 0°C for the month of May. Variability in precipitation and air temperature are predicted to increase in the future (Larsen et al., 2014). Increasing trends in PDD may be an indicator of climate trends, resulting in changes in the surface energy balance and impacting snowmelt magnitude and timing (Callaghan et al., 2011; Foster et al., 2008; Liston & Hiemstra, 2011).

Peak snowmelt discharge is the first component of snowmelt discharge analyzed. Peak snowmelt discharge is defined at the maximum discharge or streamflow of a river system associated with snowmelt. The snowmelt runoff peak is often the largest hydrologic event of the year for the Upper Kuparuk with rain driven storms resulting in smaller discharge peaks (McNamara et al., 1998).

The date of occurrence of peak snowmelt discharge is a second component of snowmelt discharge analyzed. Due to the limited long term monitoring of discharge in the Alaska Arctic there is limited observational studies on the timing of snowmelt runoff in headwater basins (Hinzman et al., 2005). Snowmelt has been shown to be occurring earlier in several larger Arctic Eurasian rivers and in the Kuparuk River (Hinzman et al., 2005; Peterson et al., 2002; Semmens & Ramage, 2013).

The final component of snowmelt discharge analyzed is the volume of snowmelt runoff. Volume of snowmelt runoff is the sum of the discharge attributed to snowmelt. Without examining each year's snow cover, temperature, and precipitation there is a degree of subjectivity in choosing a method for seasonal hydrograph separation. The hydrograph separation into snowmelt and summer from 1996 to 2014 was previously completed by WERC staff using the change in slope of the logarithmic discharge to indicate the end of snowmelt

(Kane et al., 2004, Geick, R.,Personal communications, 2018). Hydrograph separation was completed for 2015 using the same process.

Cumulative rainfall is representative of antecedent surface and subsurface storage an important component of the water budget. In areas of continuous permafrost, subsurface storage capacity is limited by the depth of the active layer (Kane et al., 2004). During snowmelt the active layer is frozen further decreasing the available subsurface storage during snowmelt. Throughout the summer the depth for the active layer continuous to increase, attenuating the runoff response and increasing subsurface storage (Kane et al., 2008; McNamara et al., 1998). Rainfall is correlated to the antecedent surface storage available within a basin for the next year's snowmelt, especially in low gradient coastal watersheds (Stuefer et al., 2017). Gauged precipitation in the Arctic has been shown to have systematic sampling errors that can result in significant under catchment (Goodison et al., 1998). There are recommended correction factors that can be applied to account for the under catchment (Yang et al., 1998), however, for the purpose of this study no corrections were applied to gauged rainfall.

Seasonal maximum snow water equivalent (SWE) is a primary component of the water balance and a driving variable for snowmelt runoff. Years of high SWE have a higher potential to produce large snowmelt runoff. Snow accumulation in the Arctic begins in September and continues through May some years. As with the rest of the Arctic, wind transport of snow is prevalent and snow distribution is spatially diverse throughout the Upper Kuparuk basin (Sturm & Stuefer, 2013). The SWE accuracy is 10% due to errors associated with data collection methods (Stuefer, 2013).

## 4.2 Trend Analysis- Mann Kendall Test

The non-parametric Mann-Kendall statistical test was performed on the processed hydrometeorological variables to determine monotonic trends. The Mann-Kendall test was chosen based on its ability to accommodate non-normally distributed data and missing values in time series, both present in the Upper Kuparuk data set. Previous hydrologic work has used Mann-Kendall to detect trends hydrometeorological data in northern Canada (Déry & Wood, 2005).

The Mann-Kendall test uses an ordered time series to test the null hypothesis, $H_o$, that the data series is independent (no trend) and identically distributed against the alternative

hypothesis, $H_A$ (Mann, 1945) . $H_A$, is the upward or downward trend in the data (Mann, 1945). The Mann-Kendall test analyses the sign difference between data points, comparing each value to those preceding it.

Each hydrometeorological variable time series was ordered $x_1, x_2, \ldots x_n$. The difference between $x_j$ and $x_k$ is determined where $j > k$. The sign of the differences is then taken.

$$\text{sgn}\,(x_j - x_k) = 1 \text{ if } x_j - x_k > 0$$

$$\text{sgn}\,(x_j - x_k) = 0 \text{ if } x_j - x_k = 0 \text{ or cannot be assessed or determined}$$

$$\text{sgn}\,(x_j - x_k) = -1 \text{ if } x_j - x_k < 0$$

The Mann Kendall statistic S is computed using the following equation:

$$S = \sum_{k-1}^{n-1} \sum_{j-k+1}^{n} \text{sgn}\,(x_j - x_k) \qquad (2)$$

If S is positive, then measurements made at a later time step are greater than those made early. A negative S value indicates that smaller measurements were made later in time. No trend is indicated by small absolute values of S. The test statistic $\tau$ is calculated using the following equation:

$$\tau = \frac{S}{\frac{n(n-1)}{2}} \qquad (3)$$

$\tau$ ranges from 1 to -1. $H_o$ is rejected when the difference between S and $\tau$ is significantly different from zero (Mann, 1945; Meals et al., 2011; Salas, 1993). A value of H=1 reject $H_o$, while H = 0 indicates insufficient evidence to reject $H_o$. For the purposes of this study significance value of 0.05 was used for all variables tested. A two-tailed probability using a normal cumulative distribution function and $\tau$. The test was performed in MATLAB R2018 (Fatichi, 2009).

## 4.3 Snowmelt Runoff Model (SRM)

SRM was used to simulate hydrographs for selected years in the Upper Kuparuk. An initial year was used to calibrate a set of parameters that were then used on an independent test year to determine the feasibility of modeling and forecasting snowmelt runoff using SRM in the Upper Kuparuk.

### 4.3.1 Model Year Selection

As previously mentioned the timing and amount of precipitation occurring in the Arctic is predicted to shift towards warmer and wetter spring months with an increase in extreme events (Larsen et al., 2014). Modeling an extreme year to capture some of the future variability will allow for understanding of the applicability of the SRM in the future scenarios including forecast and climate change. To determine the years to calibrate and model with the SRM, years of interest were identified using the following strategy.

Mean, standard deviation, and coefficient of variation (CV) of the hydrologic and meteorologic variables were calculated and examined for the Upper Kuparuk for the available period of record. Years with multiple variables outside of one standard deviation were identified as possible extreme years to calibrate SRM for the Upper Kuparuk. Further examination into patterns in hydrologic variables that could contribute to extreme years was then conducted, such as the rainfall the previous summer.

Identified extreme years were then compared to hydrologic variables from Imnavait (WERC and NRCS) and Kuparuk River (USGS) (Table A2 and Table A3), to examine and understand regional patterns. Years with multiple sites and variables outside of one standard deviation were considered to indicate a regional pattern and more weight was given to such years for modeling.

4.3.2 SRM Inputs

The Upper Kuparuk DEM was analyzed in ArcGIS to select hydrologic response unites (zones) for SRM. Three zones were used for the Upper Kuparuk watershed shown in Table 3. Zone selection was based on physical properties of the watershed (Figure 3).

Zone 1, valley, is associated with the stream channel and composed of riparian vegetation; willows and shrubs. The elevation of Zone 1 ranges from 738 m - 900 m and is 34.3 $km^2$ (Table 3). Zone 2, rolling foothills, is the largest of the three zones (73.8 $km^2$) and was delineated based on terrain and snow deposition patterns. Snow drift persistence in the zone 2 results in a longer ablation period compared to the valley region. Zone 2 ranges in elevation from 901 m – 1097 m. Zone 3, mountains, is composed of the upper portions of the watershed and is characterized by mountainous terrain including rocky outcrops and steeper terrain (Table 3). Zone 3 snow deposition is influenced by wind and sublimation. The elevations of Zone 3 range from 1098 m- 1519 m and is 22.4 $km^2$ (Table 3).

*Table 3. Three zones used in the Snowmelt Runoff Model summary information.*

| | **Area ($km^2$)** | **Mean Elevation (m)** | **Range (m)** | **Average Slope %** |
|---|---|---|---|---|
| **Zone 1 "Valley"** | 34.3 | 840 | 738 - 900 | 5.8 |
| **Zone 2 "Foothills"** | 73.8 | 994 | 901 - 1097 | 7.6 |
| **Zone 3 "Mountains"** | 22.4 | 1189 | 1098 - 1519 | 17.6 |

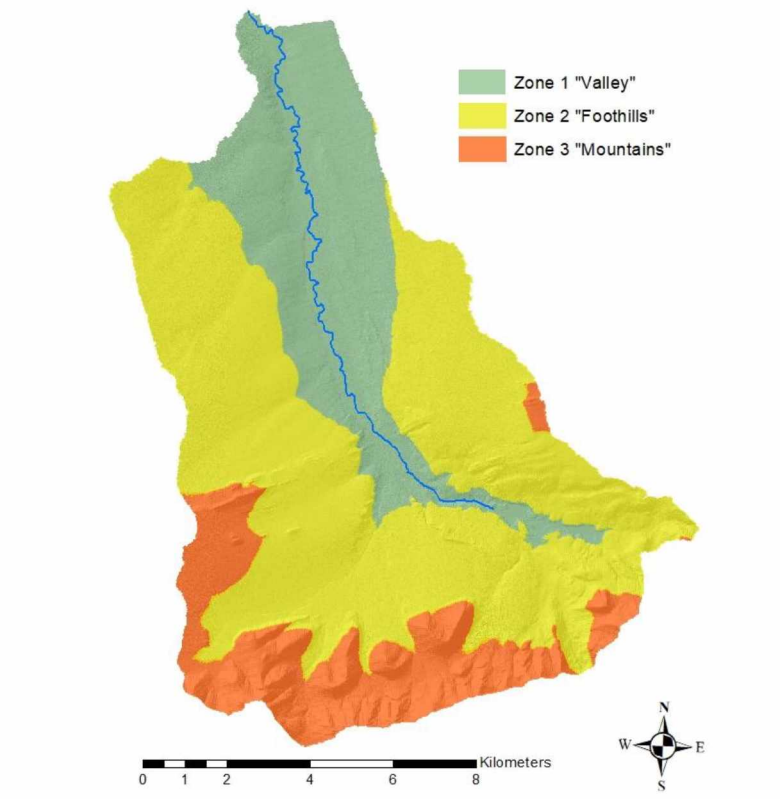


*Figure 3. The three zones (hydrologic response units) based on elevation and physical characteristics of the Upper Kuparuk Watershed used in the Snowmelt Runoff Model.*

4.3.2.1 Air Temperature and Precipitation

Due to the size and limited meteorological network within the Upper Kuparuk basin, the three elevation zones all used the same temperature and precipitation. Daily air temperature and precipitation obtained from the UKmet station were used for the primary model inputs. Daily 15-minute precipitation measurements were summed for a daily value while air temperature was averaged.

4.3.2.2 Snow Depletion Curves

The third SRM input is a snow depletion curve (SDC) for each zone. SDCs are a function the proportion of snow covered area (SCA) and time. The SDC is one of the components that provides the quantity of available water for snowmelt runoff in SRM. MODSCAG images were used to determine SDCs. Daily MODSCAG images were downloaded for years of interest. Each

scene was projected into WSG 1984 UTM Zone 6N, MODSCAG originally uses a sinusoidal projection. The images were then clipped to each individual zone.

Processed and clipped images were evaluated for the percentage of cloud cover in each zone. For this study, days with less than 20% cloud cover for each zone were used to create SDCs, all other days were excluded. The percentage of snowmelt in between days with greater than 20% cloud cover was linear decreased until the next day without cloud obstruction. Computed SDC were compared to WERC measured snow ablation measurements from the Upper Kuparuk and Imnavait, if available, or to NRCS snow depth depletion measurements.

### 4.3.3 SRM Parameters

Recommended values from the SRM manual were used for initial parameterization of lag time, temperature lapse rate, and critical temperature. Degree-day factor, runoff coefficients, and recession coefficients required basin specific values for initial model runs.

The degree-day factor is used to relate the air temperature to the amount of melt water available for runoff in the snowpack. The degree-day factor is not constant and varies with physical snow properties. The SRM model allows for the degree-day factor to be changed daily, although it is recommended to only change once a month. A single degree-day factor was used for the entire period of analysis due to short snowmelt periods, one to three weeks. Degree-day factor selection is required for each individual year modeled.

A review of previous temperature degree day modeling done in Imnavait watershed found degree-day factors ranging from 0.12 to 0.39 cm $d^{-1}C^{-1}$ depending on the year, with optimal values of 0.27 cm $d^{-1}$ $C^{-1}$ (1997) and 0.35 cm $d^{-1}C^{-1}$(1991) showing the high degree of variability possible (Hinzman & Kane, 1991; Kane et al., 1997). In a review paper compiled degree-day factors from studies around the world, the range found was highly variable, 0.25 to 1.16 cm $d^{-1}C^{-1}$ depending on elevation, glaciation, and meteorological patterns of the area (Hock, 2003). In non-glaciated sites the range was 0.25 to 0.55 cm $d^{-1}C^{-1}$ (Hock, 2003). A range of 0.03 to 0.76 cm $d^{-1}C^{-1}$ was found for all SRM studies conducted prior to 1986 (Martinec & Rango, 1986). Degree-day factors were optimized for each year by comparing the measured basin wide SWE values to the snowmelt produced in the SRM model.

Initial runoff coefficients for rain and snow were calculated from previous work done in the Upper Kuparuk (Kane et al., 2012; Kane et al., 2004; Youcha et al., 2018). To calculate runoff coefficients the total volume of runoff associated with the type of precipitation was divided by the total amount of each type of precipitation. The average runoff coefficients from 1996 to 2015 were used for both snow and rain, 0.51 and 0.78 respectively. Further optimization of the runoff coefficients was done during model calibration.

The recession coefficient (k) is a crucial parameter and serves as the transfer function for SRM with *(1-k)* determining the amount of snowmelt (or rainfall) immediately contributed to runoff and determines the shape of the recession during times with no new input of snowmelt or rainfall. Although the SRM manual refers to k as a coefficient, the recession coefficient is a function that varies with time based on discharge with two coefficients, x and y, and will thence forth be referred to as the recession function.

The recession function is not constant, decreasing with increasing discharge according to the following equation (Martinec et al., 2008):

$$k_{n+1} = x * Q_n^{-y} \tag{4}$$

where *n* is the time step, *Q* is discharge, and *x* and *y* are constants.

Historical analysis of discharge, plotting $Q_n$ verse $Q_{n+1}$ during periods of true runoff recession and the lower envelope line or medium line of all data to determine k values (Figure 4). The constants x and y are then determined using the following set of equations:

$$k = \frac{Q_{n+1}}{Q_n} \tag{5}$$

$$k_1 = x * Q_1^{-y} \tag{6}$$

$$k_2 = x * Q_2^{-y} \tag{7}$$

$$logk_1 = \log x - y * log\ Q_1 \tag{8}$$

$$log\ k_2 = logx - y * log\ Q_2 \tag{9}$$

The recession described and used by SRM is not the typical recession used in other hydrologic applications (Equation 10) but instead follows Equation 11.

$$Q_n = Q_0 * k^n \tag{10}$$

$$Q_n = x^{\frac{1}{y}} \left( \frac{Q_0}{x^{\frac{1}{y}}} \right)^{(1-y)^n} \tag{11}$$

Where $Q_0$ is the initial discharge, $Q_n$ is the discharge after n days, and x and y are the constant from Equation 4.

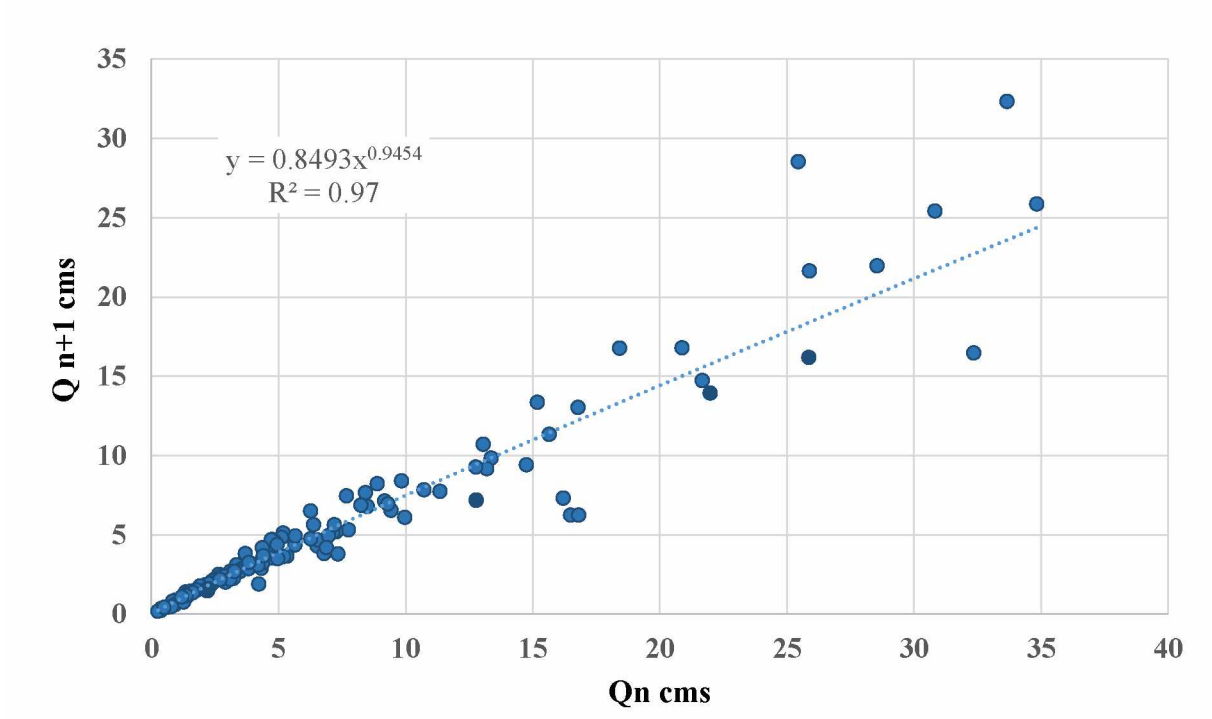


*Figure 4. Recession graph of historical snowmelt runoff. The envelope line shown were used to select initial x and y coefficients to calculate the k function. Rainfall coefficients were calculated with the same method.*

Another important basin characteristic corresponding to the recession function is the basin's rainfall threshold, which is entered in SRM at the start of each simulation and held constant by the model throughout the simulations. The rainfall threshold is the amount of rainfall needed to initiate a "heavy rainfall response" in the model, where the k function is calculated by (Equation 4) multiplying $Q_n$ by four for the five days following a precipitation event exceeding the rainfall threshold. This results in a lower k and greater (1-k), see Equation 1. The rainfall threshold is not applied to snowmelt in the current model design and rapid snowmelt does not trigger the mechanism.

4.3.4 Model Evaluation and Accuracy

SRM performance was evaluated using two different metrics computed within SRM (1) the coefficient of determination, Nash-Sutcliffe coefficient ($R^2$), and (2) the volume difference ($D_v$) between the measured discharge and model computed discharge (Martinec et al., 2008). The coefficient of determination is computed by the model with the following equation:

$$R^2 = \frac{\sum_{i=1}^{n}(Q_i - Q_i')^2}{\sum_{i=1}^{n}(Q_i - \bar{Q})^2} \quad (12)$$

Where $Q_i$ is the measured daily discharge; $Q_i'$is the computed daily discharge; $\bar{Q}$ is the average measured discharge for the given year or snowmelt season; and n is the number of daily discharge values (Martinec et al., 2008).

Volume difference is calculated by the model using the following equation:

$$D_v(\%) = \frac{V_R - V_R'}{V_R} * 100 \quad (13)$$

Where $V_R$ is the measured runoff volume for the runoff period and $V_R'$ is the computed runoff volume of the runoff period.Visual inspection of the SRM computed hydrograph compared to the measured hydrograph was also used to determine the accuracy of the model for peak timing and fit.

# 5. Results

## 5.1 Trends and Variability in Observational Hydrometeorological Data

The summary statistics for the Upper Kuparuk are shown in (Table 4). The six hydrometeorological time series for the Upper Kuparuk all reported a value of zero for $H_o$, indicating no upward or downward trend using the Mann-Kendall test (Table 4). The calculated p values range from 0.54 to 0.91 for the six variables.

A high degree of variability was seen in several of the variables. Peak snowmelt discharge and May PDD have the largest degree of variation with CV values both equal to 0.58. The date of occurrence of peak discharge has the smallest variation with a mean of May 25 (145), standard deviation of 7 days, and CV of 0.05. Snowmelt volume ranges from 8 mm to 113 mm with a CV of 0.30. The earliest occurrence day is May 13 (133) in 1995 and the latest June 7 (158) in 2000. Cumulative rainfall for the watershed has a mean of 207 mm with a standard deviation of 71 mm and a CV of 0.34. SWE has a mean value of 11.3 cm and a CV of 0.28.

The highest SWE and warmest May are seen in 2015, 17.6 cm, and 141 PDD respectively (Figure 5). The highest snowmelt peak discharge for the Upper Kuparuk is in 2011, 50.0 cms, with the second highest seen in 2015, 44.6 cms. The lowest discharge is 3.8 cms in 1999 corresponding to the lowest SWE on record 5.4 cm. The largest snowmelt runoff volume is in 2003 with the lowest volume, 8 mm, in 2008. The largest rainfall is seen in 1997 with 359 mm. the lowest rainfall, 62 mm, occurs in 2007. The snowmelt hydrometeorological time series highlight the large range of natural variability in snowmelt discharge and precipitation inherit to Arctic watersheds.

*Table 4. Summary table of hydrometeorological variables for Upper Kuparuk including Mann-Kendall results. A significance level of 0.05 was used in the Mann-Kendall test.*

| | Date Range | Units | Sample Size | Mean | Standard Deviation | Coefficient of Variation | Min | Max | Mann-Kendall Results | |
|---|---|---|---|---|---|---|---|---|---|---|
| | | | | | | | | | H | p |
| **Snow Water Equivalent** | 1996-2017 | cm | 21 | 11.0 | 3.1 | 28.4 | 5.4 (1999) | 17.6 (2015) | 0 | 0.88 |
| **Cumulative Rainfall** | 1995-2017 | mm | 20 | 207 | 71 | 34.3 | 62 (2004) | 359 (1997) | 0 | 0.54 |
| **Peak snowmelt discharge (Qp)** | 1993-2017 | cms | 25 | 22.4 | 13.0 | 57.9 | 3.84 (1999) | 50 (2011) | 0 | 0.56 |
| **Qp Occurrence Date** | 1993-2017 | Julian | 25 | 145 | 7 | 4.8 | 133 (1995) | 158 (2000) | 0 | 0.64 |
| **May Positive Degree Days** | 1994-2017 | C | 22 | 64.7 | 37.7 | 58.3 | 7.4 (2000) | 155.2 (2015) | 0 | 0.91 |
| **Volume Snowmelt Runoff** | 1996-2015 | mm | 20 | 63 | 26 | 30.0 | 8 (2008) | 113 (2003) | 0 | 0.67 |

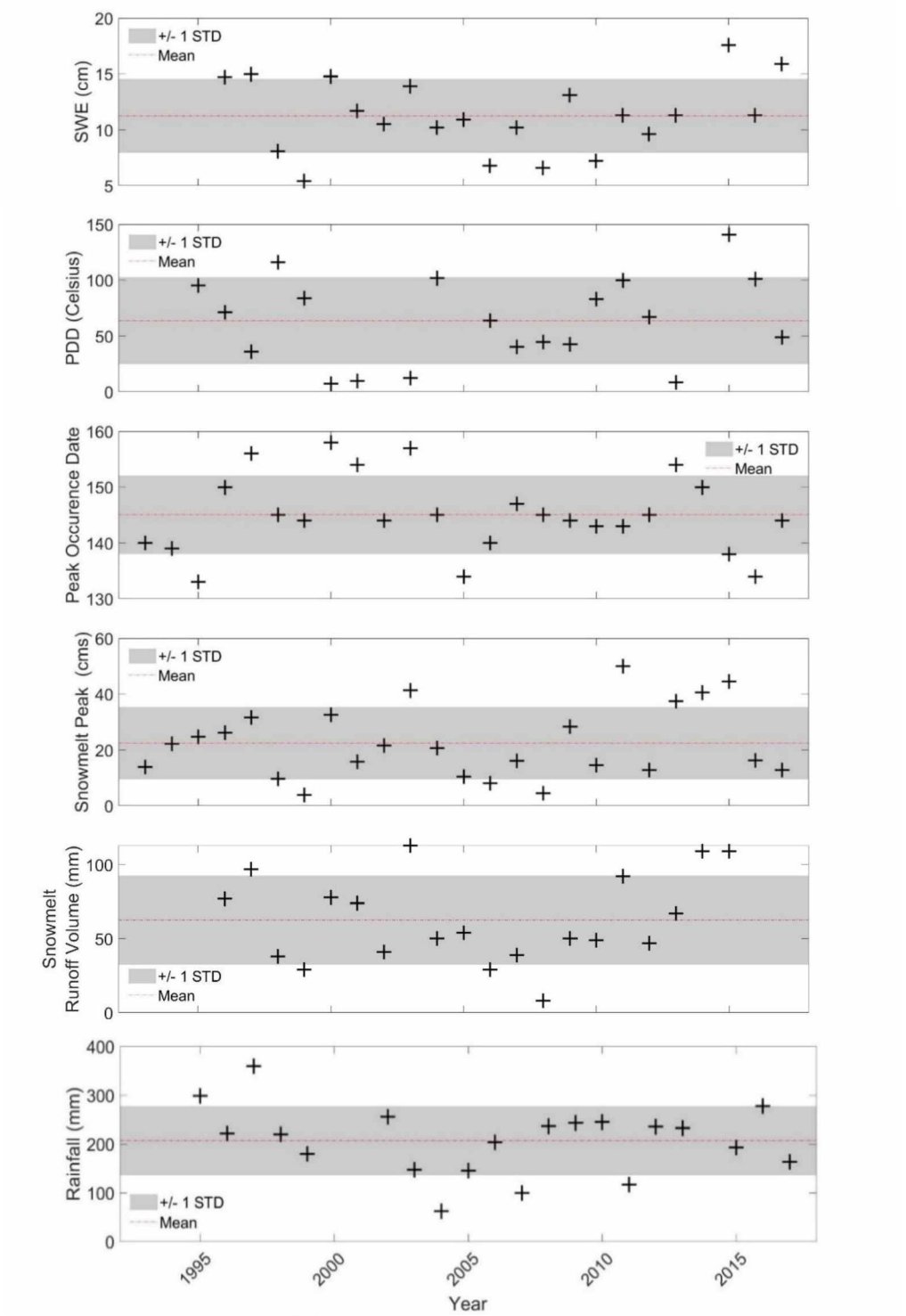


*Figure 5. Time series of hydrometeorological variables for Upper Kuparuk.*

## 5.2. Snowmelt Runoff Model

### 5.2.1 Model Year Selection

The years 2013 and 2015 were selected for modeling based on snowmelt runoff characteristic and selection criteria described in section 4.3.1.

Analysis indicates that 2015 is an extreme year in the Upper Kuparuk. Out of the five available hydrometeorological variables, four are outside of one standard deviation from the mean. Results show that in May 2015, rapid snowmelt associated with the largest SWE and May PDD on record, produced one of the earliest $Q_p$ (May 18) nd largest volumes of snowmelt runoff (101 mm) (Figure 5 and Figure 6).

Regional trends support the identification of 2015 as an extreme year. Imnavait watershed experienced the warmest May on record with 144 positive degree days (Table A2). Imnavait also reports the highest SWE in 2015, 19.8 cm during 1985 – 2017 time period. The Kuparuk River USGS gaging station had a discharge of 2458 cms with the second earliest date of occurrence, May 21(141), for the period of record (1985-2017). The 2015 Kuparuk peak snowmelt discharge is the third largest for the 47-year record, with 2013 having the same discharge (Table A3). On a larger Arctic perspective, the six largest Eurasian rivers in 2015 for the first 7 months of the year had a combined discharge 10% greater and five days earlier than the 1980-1989 average (Holmes et al., 2015).

2013 was also identified as an extreme year for the Upper Kuparuk but only had three out six variable outside of one standard deviation, May PDD, peak discharge, and occurrence date (Figure 6). 2013 has the second lowest May PDD on record, 8.6 PDD, which corresponds to one of the latest snowmelt peak discharge occurrence for the period of record, June 3 (154). Unlike 2015, basin-wide SWE is average during 2013 at 11.3 cm. The magnitude of the discharge produced in 2015 and 2013 are of similar magnitude despite the conditions leading up to snowmelt are different between the two years. 2013 had a snowmelt peak discharge of 37.4 cms.

On a regional scale in 2013, the highest peak discharge in Imnavait occurred on May 29, 2013 (149) with a discharge of 2.0 cms and the second largest SWE was reported, 19.3 cm. (Table A2). 2013 produced the same discharge as 2015 at the Kuparuk River near Deadhorse, AK, 2458 cms with the 2013 occurring 13 days later than in 2015, June 4 (155).

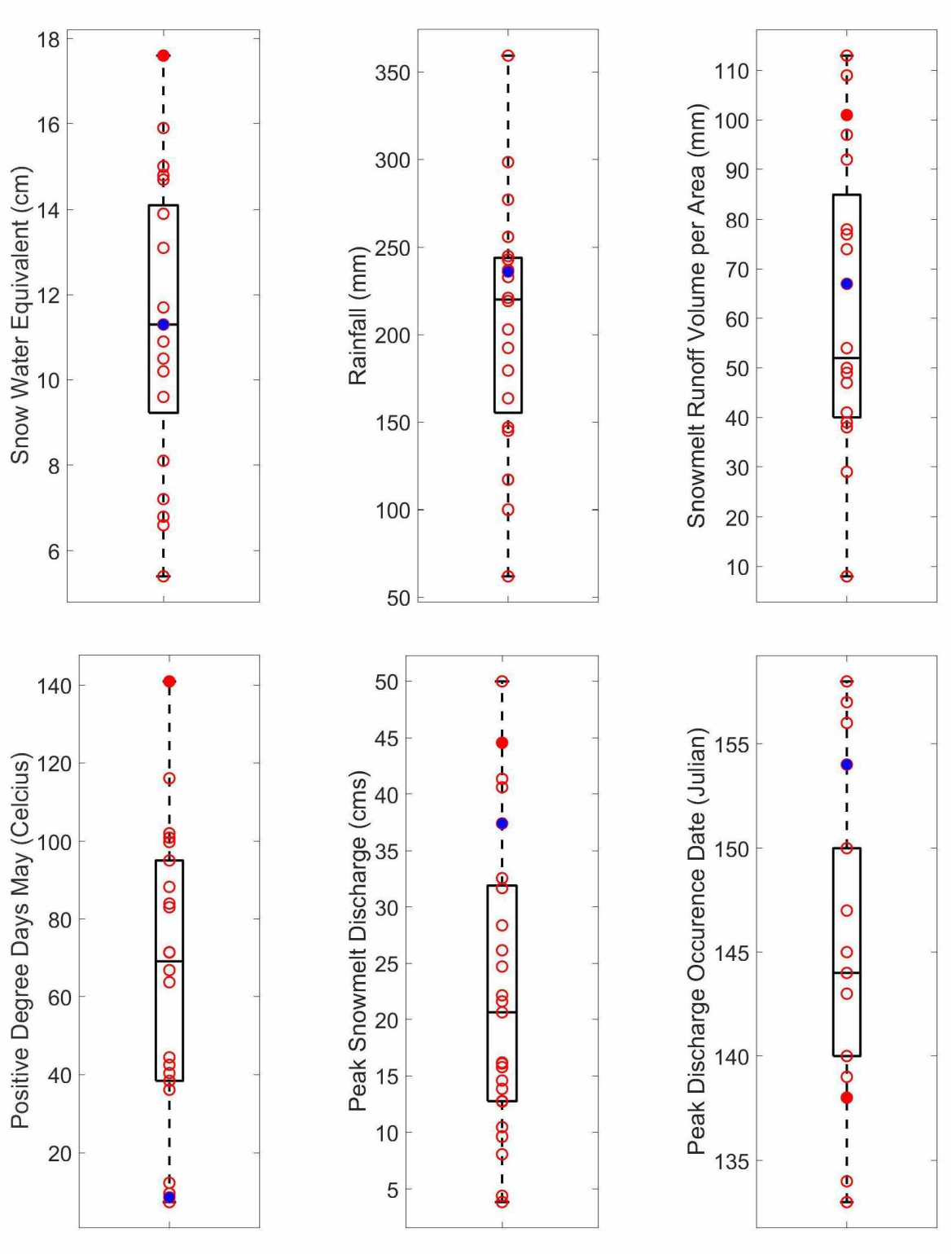


*Figure 6. Box and whisker plots of the hydrometeorologic variables in the Upper Kuparuk. 2015 (solid red) and 2013 (solid blue) were identified as model years based on snowmelt characteristics. The box shows the range of values with the median value surrounded by a rectangle composed of the 25$^{th}$ and 75$^{th}$ quartile.*

5.2.2. Model Parameters

2015 was used to calibrate a set of parameters for SRM application in the Upper Kuparuk watershed show in Table 5. Calibrated parameters were then applied to 2013 as a test year.

*Table 5. Optimized SRM parameters for the Upper Kuparuk watershed.*

| **Parameter** | | |
|---|---|---|
| **Degree Day Factor (a)** | | Year Dependent |
| **Temperature Lapse Rate (C per 100 m)** | | None |
| **Critical Temperature ($T_{CRIT}$ °C)** | | 1 |
| **Rainfall Contributing Area (RCA)** | | 0 |
| **Lag Time (hours)** | | 18 |
| | **Snow** | **Rain** |
| **X Recession Constant** | 0.849 | 0.92 |
| **Y Recession Constant** | 0.155 | 0.165 |
| **Runoff Coefficient** | 0.90 | 0.78 |

The initial runoff coefficient for snow (0.51), calculated from measured runoff and SWE in 2015, produced poor simulation results during calibration with 2015. Through model simulations the runoff coefficient was increased (Table 6). The optimized runoff coefficient found, 0.90, is outside the range of the historically calculated values in the Upper Kuparuk watershed 0.14 to 0.74. Runoff coefficients are documented to be higher in areas underlain with permafrost due to the limited subsurface storage available. Snow runoff coefficients from the entire Kuparuk basin from 1993 to 1997 report an average value of 0.86, similar to the optimal value used, 0.90 (Lilly et al., 1998). The initial rain runoff coefficient, 0.78, preformed favorably and did not need to be adjusted during calibration.

*Table 6. Model simulations to calibrate the runoff coefficient for snow in 2015.*

| | Snowmelt 2015 | | | |
|---|---|---|---|---|
| **Runoff Coefficient (Snow)** | **0.51** | **0.65** | **0.78** | **0.9** |
| **Measured Runoff Volume (10^6 $m^3$)** | 16.35 | 16.35 | 16.35 | 16.35 |
| **Computed Runoff Volume (10^6 $m^3$)** | 8.0 | 10.9 | 13.7 | 17.2 |
| **Volume difference %** | 51.1 | 33.4 | 16.0 | -5.1 |
| **Coefficient of Determination ($R^2$)** | 0.37 | 0.6 | 0.73 | 0.76 |

The degree-day factor required independent calibration for both model years. Based on the computed SDCs and measured SWE values degree-day factors of 0.44 cm $d^{-1}C^{-1}$ (2015) and 0.30 cm $d^{-1}C^{-1}$ (2013) were found. The zonal daily snowmelt results from 2015 are shown in Figure 7. Zone 1 and 2 yield the same total snowmelt, 17.7 cm, while Zone 3 yields 12.9 cm. The WERC snow survey measured a value of 17.6 cm for the basin-wide SWE average.

In 2013, measured basin-wide average SWE in 2013 was 11.3 cm. The daily snowmelt results from SRM calculate the following totals: Zone 1 11.3 cm, Zone 2 12.0 cm, and Zone 3 12.5 cm (Figure 8). Zone 2 and 3 snowmelt totals are greater than the measured SWE value although the difference between the three zones is 1.2 cm, an amount that is within the measure error margin associated with the ground-based snow surveys. The lower snowmelt seen in Zone 3 in 2015 could be attributed to wind transport and sublimation that occurs in the upper mountainous regions of the watershed yielding less available snow for melt. However of the six locations used in the annual average SWE calculations, none are in the boundary of zone 3 leading to difficulty in confirming the SWE values independently for all three zones (Figure 1).

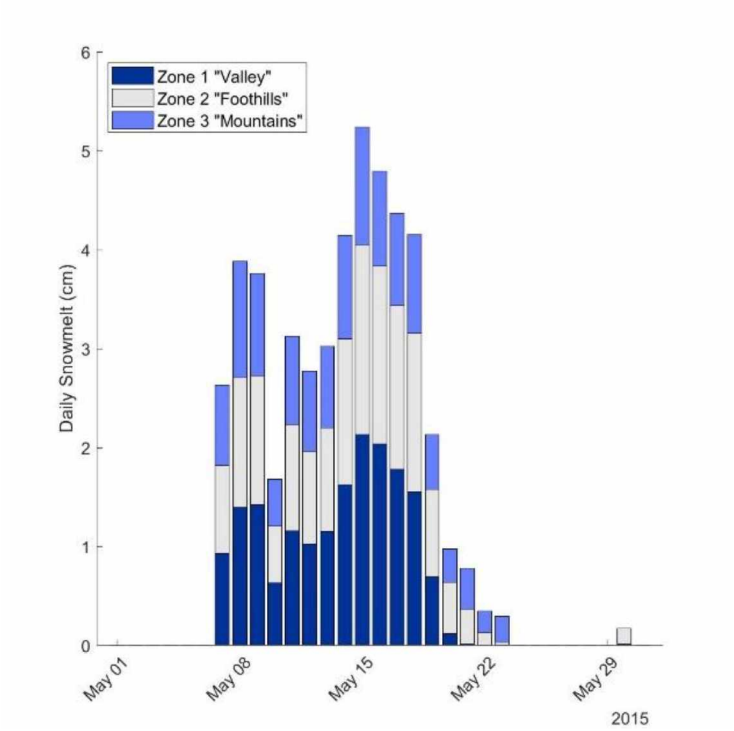


*Figure 7. Daily snowmelt (cm) during 2015 SRM simulations using an optimized degree-day factor of 0.44 cm $d^{-1}C^{-}$. Results are separated by the three zones used in SRM.*

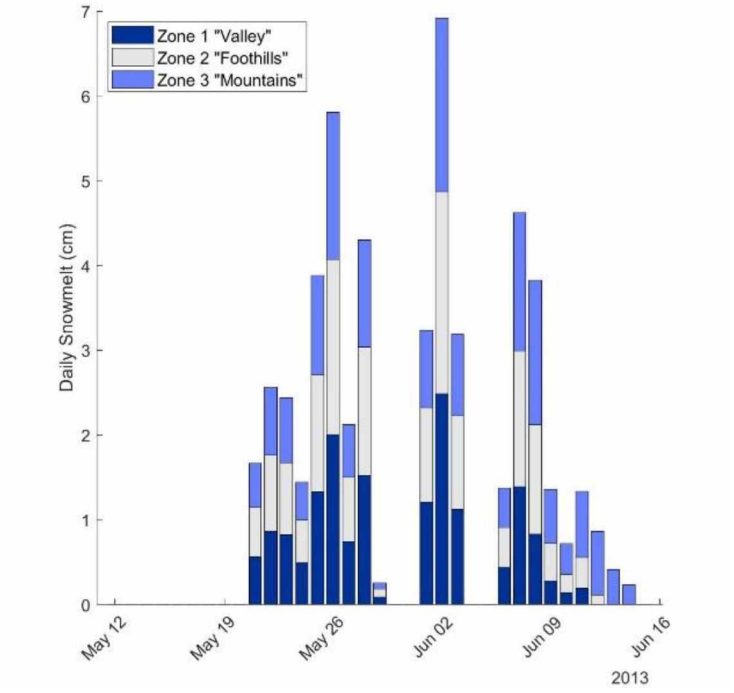


*Figure 8. Daily snowmelt (cm) during 2013 SRM simulations using an optimized degree-day factor of 0.30 cm $d^{-1}C^{-1}$. Results are separated by the three zones used in SRM.*

Another parameter that was different than the SRM default value was the temperature lapse rate. Comparison of average daily temperature from the Upper Kuparuk meteorological station, elevation 753 m, and Imnavait meteorological station, elevation 897 m, were used to determine the optimal lapse rate. This comparison for the year 2015 shows no trends between elevation and temperature in the Upper Kuparuk area that would indicate the use of a lapse rate during snowmelt (Figure 9). The lack of a temperature elevation trend was confirmed in 2013. It is recommended to not use a temperature lapse rate in the SRM for snowmelt in the Upper Kuparuk.

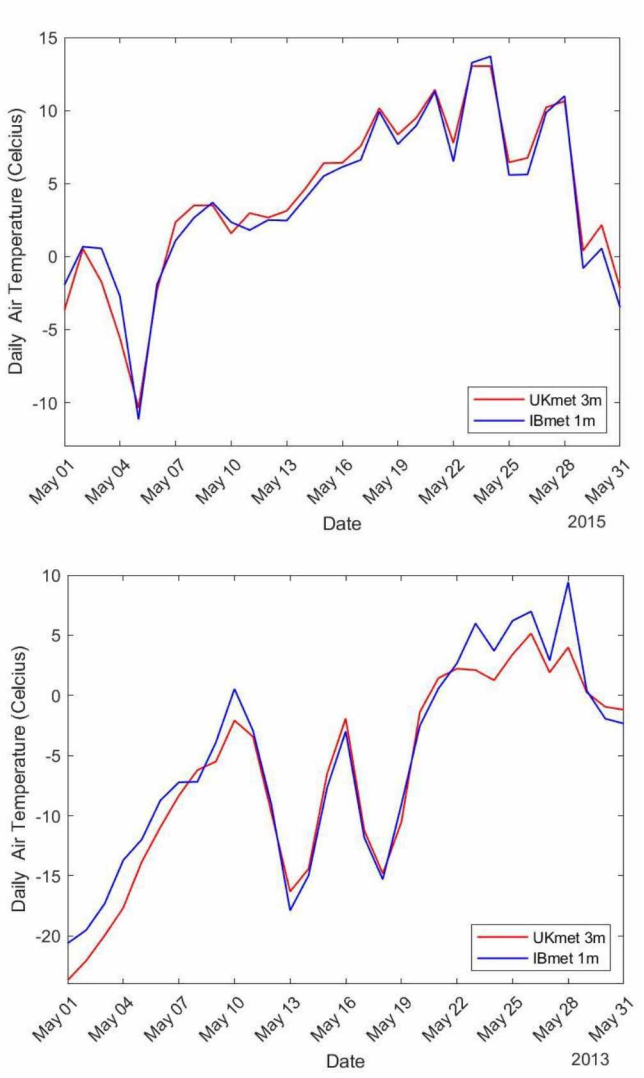


*Figure 9. Comparison of average daily air temperature for Upper Kuparuk meteorological station at 3 m and Imnavait meteorological station (IBmet) at 1 m for the snowmelt duration in (top) 2015 and (bottom) 2013.*

Utilizing snowmelt runoff recession from 2005-2015, as described in section 4.3.3, the x and y constants for the snow runoff coefficient (function) were 0.849 and 0.155, respectively. Different constants were used for the rain runoff coefficient and calculated from rainfall recession from 2005-2015, 0.92 (x) and 0.165 (y). The use of different constants allows for different transfer functions (runoff coefficient) to represent the different controls on runoff response between the two runoff regimes, snowmelt and rainfall. During snowmelt runoff response is controlled by snowpack, frozen ground, and the timing of snowmelt. In contrast the rainfall runoff response is driven by precipitation intensity and amount, the depth of the active layer, and the available subsurface storage. The same constants were used for both years.

A critical temperature of 1℃ was used for this study based on temperature seen during the rainfall from the UKmet on May 30, 2015 and May 23-25, 2013. The default value is 2°C, requiring only a minor adjustment for the Upper Kuparuk.

The default lag time of 18 hours was used for both model years. The lag time is used to account for the time difference in the rise of temperature and corresponding rise in runoff. Comparison of air temperature and hydrographs showed that 18 hours was an accurate lag time.

Rainfall contributing area (RCA) initially used the default setting of 0 in both years, indicating that the snowpack had not yet ripened. Examination of the snowpack is required to determine when the change RCA to a value of 1, indicating that the snowpack has ripened. In 2015, this occurred on May 13 based on the SDCs. In 2013 a rain event ripens the snowpack on May 25.

### 5.2.3 Snow Depletion Curve and MODSCAG

The SDCs for 2015 and 2013 show good correlation to the available ablation SWE measurements (Figure 10 and Figure 11). SWE ablations was measured daily in May-June 2013, whereas in 2015 SWE ablations measurements were reconstructed from NRCS snow data. The snowmelt during 2015 occurs from May 6 to May 23, 16 days, based on the SDCs. SDCs compared favorably to NRCS SNOTEL snow depth depletion and visual observational SCA data from Imnavait. Field observations reported a 25% SCA on May 20, 2015 and a snow-free date of May 23, 2015 in Imnavait watershed. The computed SDCs have snow-free date between May 21 (Zone 1) and May 23 (Zone 3) in 2015 (Figure 10). NRCS SNOTEL reports a snow-depth of 0 cm on May 22, 2015 the same as Zone 2. The slope of the SDCs are similar to the SNOTEL

depth depletion as well indicating further confidence in the MODSCAG performance for the Upper Kuparuk during 2015 snowmelt.

In 2013, SWE ablation curves were available for both Imnavait and Upper Kuparuk for comparison. The shape of the SDC and the snow-free date compare favorable for 2013 (Figure 11). Snowmelt in 2013 occurs from May 21 to June 15, 25 days. The Upper Kuparuk SWE ablation reports a snow-free date of June 8 earlier than the Imnavait date, June 12, same as Zone 1. SDCs show Zone 2 with a snow-free date of June 13 and Zone 3 snow-free on June 15. However, there is a week lag between MODSCAG SDCs and observed SWE ablation reaching 50%. This highlights the different metrics being compared, SCA depletion (MODSCAG) versus SWE ablations.

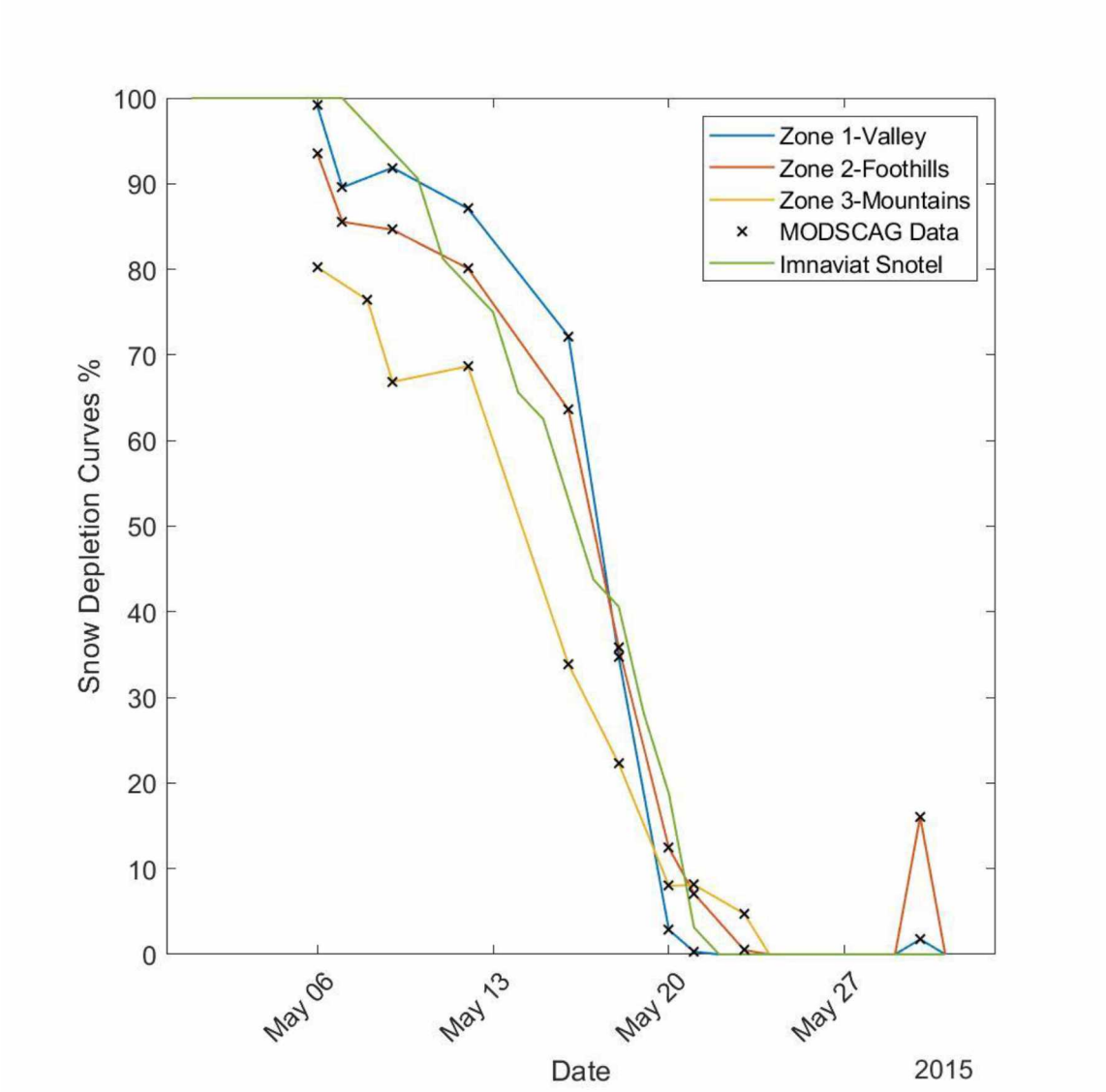


*Figure 10. 2015 snow depletion curves for the three zones. Days when MODSCAG data was available, less than 20% cloud cover, are indicated with an x. NRCS Imnavait SNOTEL was used for comparison.*

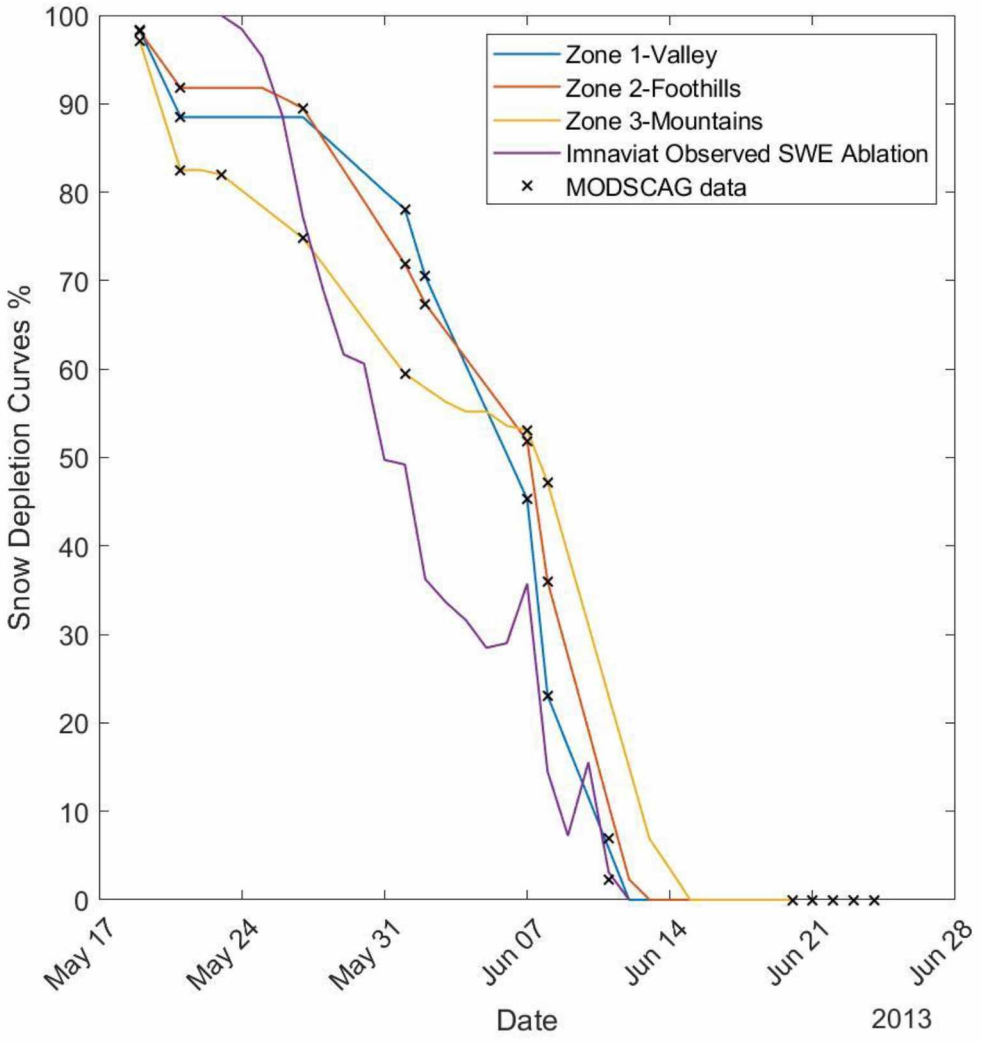


*Figure 11. 2013 snow depletion curves for the three zones. Days when MODSCAG data was available, less than 20% cloud cover, are indicated with an x. SWE ablation data was collected by WERC for both Imnavait and Upper Kuparuk SWE ablations curves and were used for comparison.*

5.2.4 Model Hydrographs

For the two selected model years, 2013 and 2015, SRM simulations were run for the snowmelt runoff period and entire open water runoff period. Results for the simulations are shown in Table 7. SRM performance was considered good for $R^2$ value greater than 0.70 and $D_v$ less than +/- 10%.

*Table 7. SRM results for the years 2015 and 2013.*

| | Open Water | | Snowmelt | |
|---|---|---|---|---|
| | **2015** | **2013** | **2015** | **2013** |
| **Measured Runoff Volume ($10^6$ $m^3$)** | 29.6 | 41.7 | 16.4 | 20.8 |
| **Computed Runoff Volume ($10^6$ $m^3$)** | 31.3 | 31.0 | 17.2 | 16.5 |
| **Volume Difference % ($D_v$)** | -5.7 | 25.6 | -5.1 | 20.8 |
| **Coefficient of Determination ($R^2$)** | 0.78 | 0.38 | 0.76 | 0.36 |

For 2015, snowmelt (May 1 - May 31) SRM yields a $D_v$ of -5.1% and an $R^2$ of 0.76 (Table 7). The snowmelt peak is underestimated with the computed discharge of 20.8 cms while the measured discharge is 33.7 cms. The timing of the peak is the same as the measured, May 18, 2015. Even with the underestimated peak runoff, SRM overestimates the volume of runoff during this period. This is due to the larger runoff during all periods except for the three days surrounding the snowmelt peak.

The entire open water period in 2015 (May 1 - September 22) has a $D_v$ of -5.7% and an $R^2$ of 0.78 (Table 7). Visual inspection of SRM hydrograph shows a strong correlation in timing and magnitude to the measured hydrograph (Figure 12). Total volume is overestimated by SRM during the open water simulation, $31.3*10^6$ $m^3$ versus $29.6*10^6$ $m^3$.

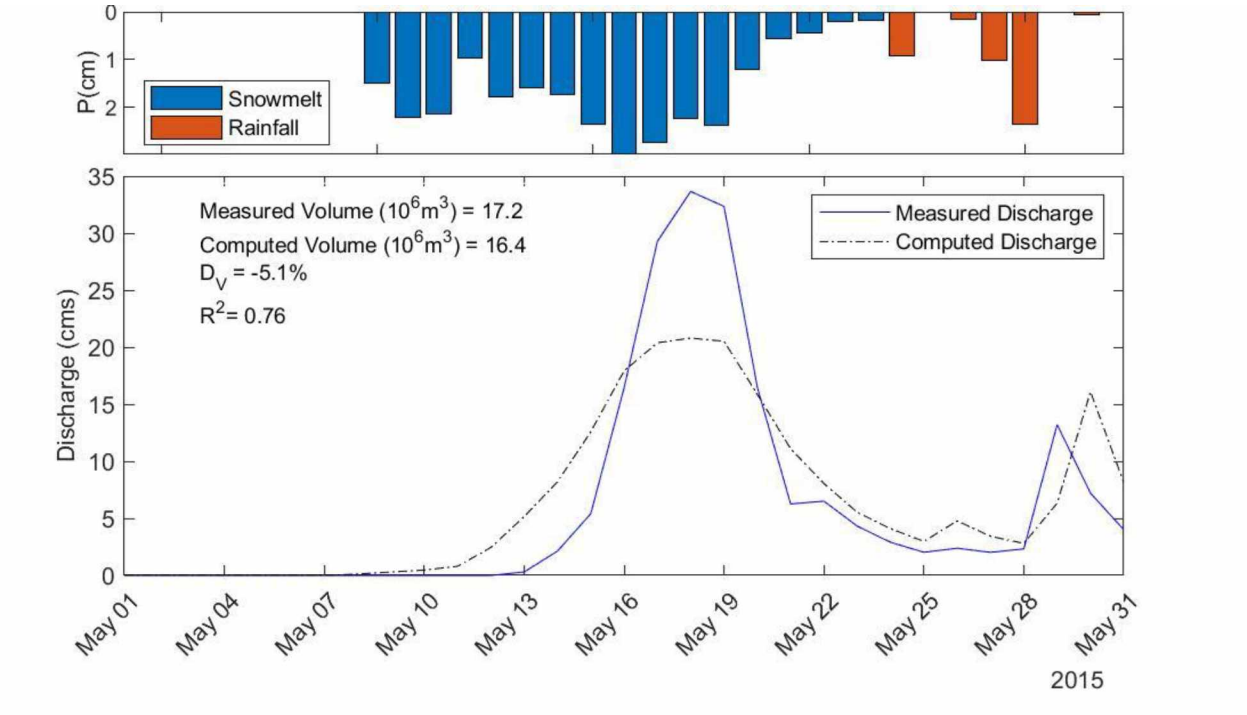


*Figure 12. 2015 SRM computed hydrograph for the snowmelt period from May 1, 2015 to May 31, 2015. Daily snowmelt and rainfall inputs in cm are displayed above hydrograph.*

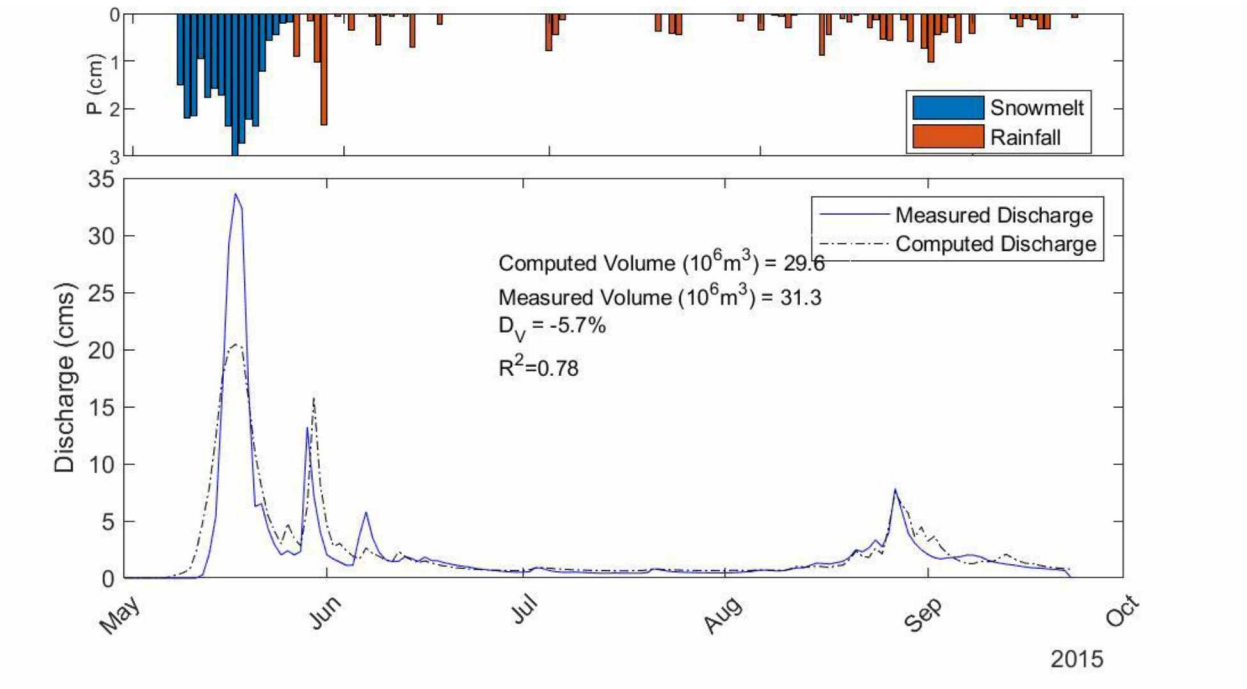


*Figure 13. 2015 SRM computed hydrograph for the open water period from May 1, 2015 to September 22, 2015. Daily snowmelt and rainfall inputs in cm are displayed above hydrograph.*

Utilizing the parameters (Table 5) from the 2015 calibration, SRM was applied to 2013 for snowmelt and entire open water periods. SRM simulations in 2013 did not perform favorably during the snowmelt and open water periods (Table 7). For the snowmelt period (May 12 - June 20) SRM produced a $D_v$ of 20.8% and an $R^2$ of 0.36. The snowmelt period in 2013 is more complex than 2015 with an extended snowmelt period due to the cooler temperatures and a rain-on-snow event on May 24-26, 2013.

SRM produces a $D_v$ of 25.6% and an $R^2$ of 0.38 for the 2013 open water (May 1 –August 31) simulations (Table 7). For 2013, SRM underestimates all of the rain events (Figure 15). Combined with the underestimation during the snowmelt period this leads to the greater volume difference in 2013 than 2015. SRM computed volume is 31.0 $*10^6$ $m^3$ while the measured volume is 41.7 $*10^6$ $m^3$. Visual inspection shows that the peak timing of measured and computed rainfall events are the same throughout the 2013 summer months (Figure 15).

Runoff initiation occurs earlier than measured runoff in both years. In 2015, snowmelt begins on May 7, but measured runoff is not initiated until May 12, a five-day lag. However, SRM initiates runoff on May 7, 2015 as soon as there is available snowmelt water. In 2013, SRM runoff initiation was six days earlier than the measured. There is no parameter within SRM that allows for storage of snowmelt and delivery at a later date.

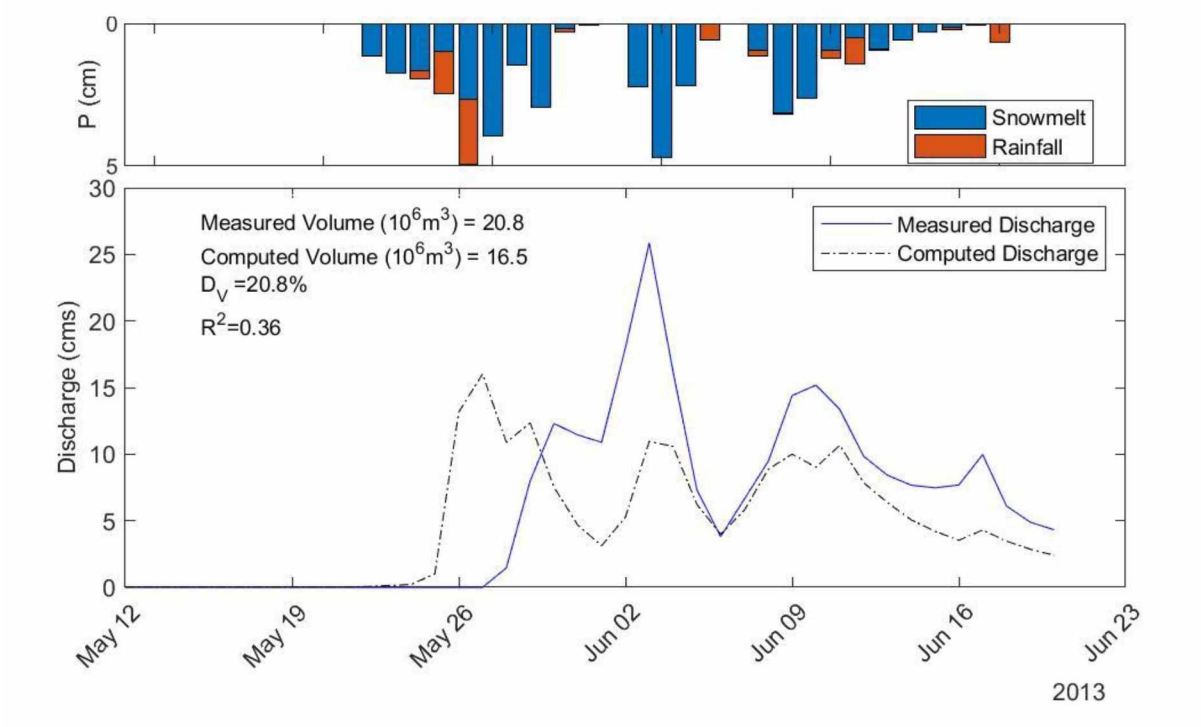


*Figure 14. 2013 SRM computed hydrograph for the snowmelt period from May 12, 2013 to June 20, 2013. Daily snowmelt and rainfall inputs in cm are displayed above hydrograph.*

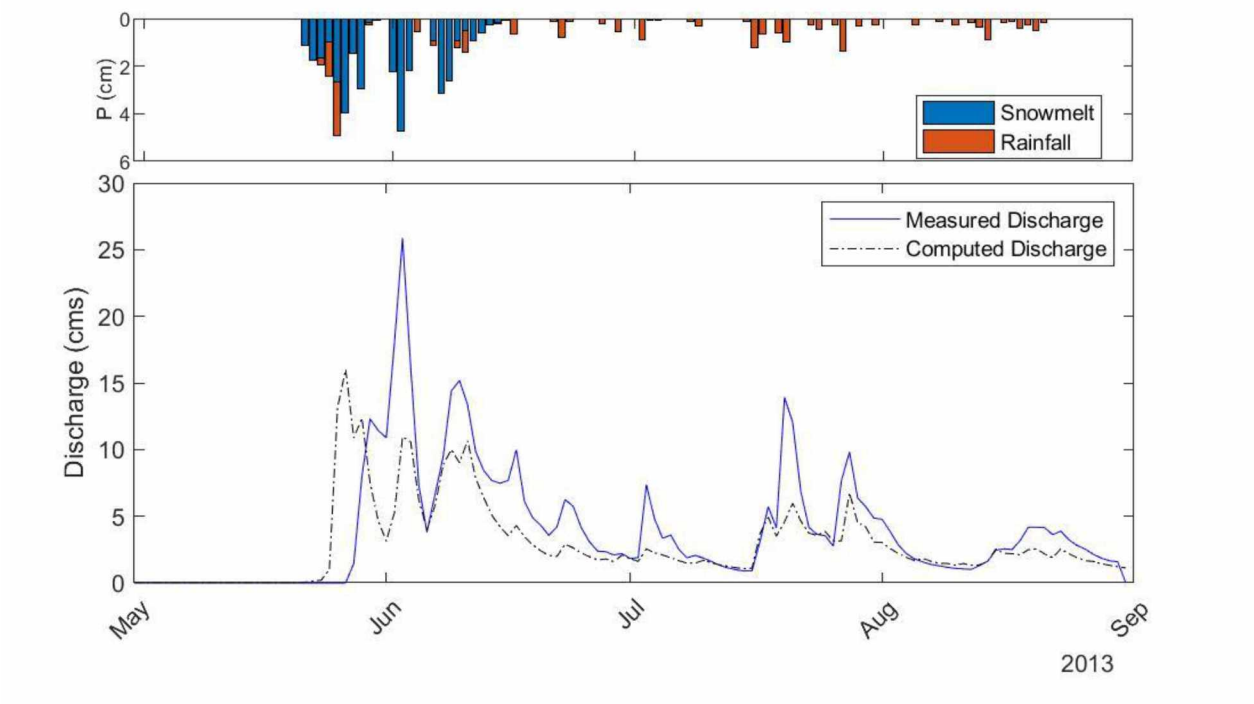


*Figure 15. 2013 SRM computed hydrograph for the open water period from May 12, 2013 to August 31, 2013. Daily snowmelt and rainfall inputs in cm are displayed above hydrograph.*

During the 2015 summer runoff period (June –August), the SRM performance is stronger than 2013 due to the rainfall threshold and the activation of the "heavy rainfall' response in SRM (See Section 4.3.3). The "heavy rainfall" response creates a runoff response with a rapid rise and decline in the hydrograph response are characteristic of the Upper Kuparuk and other permafrost impacted streams. In permafrost regions this response is due to the limited subsurface storage. Lowering rainfall threshold leads to the low recession function, k, and rapid basin responses to storms. The default rainfall threshold SRM value is 6 cm. Due to permafrost, the Upper Kuparuk and other permafrost influences basins respond to 1-2 cm of rainfall (Kane et al., 2008). A value of 1 cm was used for all model simulations.

During 2015, 35% of daily rainfall events were greater than 1 cm and initiate a heavy runoff response in SRM. Thus, k coefficient is consistently lowered throughout the summer to initiate the rapid runoff response resulting in the strong fit. In 2013 the precipitation pattern is different, none of the daily precipitation events are greater than 1 cm except for the rain-on-snow event May 24-25. During 2013, the heavy rainfall response mechanism is not activated, and the resulting hydrograph is an underestimate.

# 6. Discussion

## 6.1. Observational Trends and Variability

While no statistically significant trends in snow accumulation and snowmelt runoff were identified during 1993-2017 in the Upper Kuparuk watershed, large year-to-year variability and including extreme years are highlighted by this study. The conditions leading up to the 2015 snowmelt, warmest May and highest SWE on record, led to one of the most rapid snowmelts on record. Extreme years like 2015 lead to further interest in possible increase in variability of snow accumulation, precipitation, and air temperature in a changing climate.

The lack of statistically significant long-term trends found in the Upper Kuparuk could be attributed in part to the data deficiency of the area. The 20 to 25 years, depending on the variable, of available data from the Upper Kuparuk River area is a relatively short period of record. The closest available air temperature data with a period of record greater than fifty years to the Upper Kuparuk is Utqiagvik, AK (formerly Barrow) and Fairbanks, AK which are both located in different eco and climate regions than the Upper Kuparuk watershed. Increase in annual discharge from the Kuparuk, Sagavanirktok, and Putuligayuk rivers have been seen in part due to the greater than 50 year continuous period of record (Hinzman et al., 2005). Although this study does not examine annual discharge volume, it was hypothesized that the snowmelt discharge volume would also experience increasing trends.

Pan-Arctic trends have also shown a decrease in SWE, utilizing models and reanalysis data (Liston & Hiemstra, 2011). This same trend was not seen with the observational data from the Upper Kuparuk. However, the large SWE values seen in recent years (2015 and 2017) in Upper Kuparuk and Imnavait watershed demonstrate strong annual and regional variation present in hydrometeorological data across the Arctic. Continued monitoring and development of snow accumulation, precipitation, and air temperature time-series is needed to strengthen the dataset in the Upper Kuparuk watershed.

## 6.2 MODSCAG in the Upper Kuparuk

The relationship between SCA and runoff is critical for the SRM, providing a simplified method of assessing snow depletion at a watershed scale. There has been extensive documentation on the accuracy of MODIS snow cover products for the creation of SDCs

specifically for SRM application (Raleigh et al., 2013; Rittger et al., 2013; Steele et al., 2017; Tekeli et al., 2005). MODSCAG performed favorably for the Upper Kuparuk in 2015 and 2013 compared to the limited available ground truth data.

A high percentage of cloud-free days is needed to make SDCs in the Upper Kuparuk due to the short ablation period (7-24 days). The percentage for cloud-free MODSCAG images in 2015 and 2013 were enough to produce strong SDCs. During the snow ablation period in 2015 the percentage of usable MODSCAG days was 54% (2015) and 32% (2013), an average of all three SRM elevation zones. The lower amount of cloud-free can be attributed to the extended snowmelt period and precipitation events during snowmelt period. MODSCAG coupled with the ground-based observations and in-situ data provided enough cloud-free days to compute an accurate SDCs for the Upper Kuparuk and is a useful snow data product for hydrologic studies.

Previous work in Imnavait showed a nonlinear relationship between MODIS SCA and SWE depletion throughout the snowmelt period (Homan et al., 2011). In the work done by Homan (2011), SCA depletion was offset from SWE depletion during the initial snowmelt period in 2006, thus during the early portion of the melt period large changes is SWE yield small changes in SCA. This non-linear relationship is also seen in the 2013 MODSCAG SDCs (Figure 8), the measured SWE ablation curves from Imnavait and Upper Kuparuk result in larger initial SWE depletion compared to SDC depletion but correspond to the snow-free dates observed by MODSCAG.

## 6.3 Snowmelt Runoff Model Application

The optimized parameters found for SRM application in the Upper Kuparuk provide a starting point for future snowmelt runoff modeling and forecasting with SRM. Confidence in SRM inputs and parameters is limited by the number of meteorologic stations across elevation gradients in the northern foothills of the Brooks Range. Understanding of precipitation patterns and gradients are also limited by available data. Localized and elevation dependent storm events can be relevant in this area but were not accounted for in this study due to the lack of spatially distributed precipitation data.

Variability in SRM fit during snowmelt can be attributed to the lack of a snowmelt storage function within the SRM model structure. Available snowmelt is used in the current time

step and the next, *n and n+*, and the rest of snowmelt water is discarded. However, daily snowmelt is not immediately available for runoff. Comparison of SWE ablations and discharge measurements showed that is takes 2-10 days for snowmelt water to appear at the gauging station. SRM does not have a storage component or routing function that are seen in other hydrologic models, the only storage with the SRM is the lag time. The lag time with SRM allows for melt water delivery to be adjusted within a 24-hour period, which is insufficient for the Upper Kuparuk during the beginning of snowmelt when water delivery to the stream is limited by the remaining snowpack on the ground and in the stream channel, storage in surface depressions, and slush dams.

The runoff initiation date in both years corresponds to the first day snowmelt is produced and thus made available for runoff. SRM computed runoff began five days earlier than the measured runoff in 2015 and six days earlier 2013. The lack of a snowmelt storage function does not correspond to the physical reality of the Upper Kuparuk, especially during the early parts of snowmelt. Without a snowmelt storage function modeled snowmelt peaks will be underestimated in magnitude and runoff will initiate early as seen in both 2015 and 2013.

The underestimation of snowmelt peak discharge and early initiation of runoff by SRM are compounded in years with increased complexity during snowmelt. 2015 is a relatively simple snowmelt regime characterized by a rapid snowmelt process with consistently above freezing air temperature and no new precipitation occurred during the melt period. Many years have more complex snowmelt regimes. In 2013 a rain-on-snow event occurred at the start of the snowmelt increasing the complexity of the snowmelt regime which was poorly simulated by SRM. The analyzed hydrometeorological variables in the Upper Kuparuk indicate the snowmelt regime has high natural variability year-to-year. In the context of the changing climate increased variability in hydrometeorological variable can be expected. This could lead to more complex snowmelt regimes which would require further refinement of snowmelt models.

# 7. Conclusion

Understanding and predicting the timeline of snowmelt runoff as well as variability is essential for assessing potential impacts for vulnerable Arctic hydrologic systems with changing precipitations patterns and increasing temperatures. The exploratory trend analysis preformed for the Upper Kuparuk demonstrates the deficiency in available data and need for continued monitoring in Arctic Alaska. Snowmelt runoff in the Upper Kuparuk has high natural variability. The warmest May and largest SWE experienced during 2015 snowmelt led to an extreme snowmelt runoff year. MODSCAG coupled with the ground-based observations creates accurate SDCs for the Upper Kuparuk and is a useful snow data product for hydrologic studies. In the changing climate, increased variability in hydrometeorological variables could lead to extreme and more complex snowmelt regimes and runoff. Simplistic physically-based models, such as SRM, are useful in data sparse regions due to their data requirements. SRM does not need complex data, instead relies on readily available data, remote sensing products, and physical hydrologic basin characteristics. SRM provides a good first order approximation of snowmelt runoff in the Alaska Arctic and can be used as a tool to protect infrastructure, understand climate change, and for land management.

# References


Adam, J. C., Hamlet, A. F., & Lettenmaier, D. P. (2009). Implications of global climate change for snowmelt hydrology in the twenty-first century. In *Hydrological Processes*. https://doi.org/10.1002/hyp.7201

Alaska Water Science Center; USGS; US Department of the Interior. (n.d.). USGS 15896000 KUPARUK R NR DEADHORSE AK. Retrieved November 15, 2017, from https://waterdata.usgs.gov/ak/nwis/inventory/?site_no=15896000&agency_cd=USGS

Arp, C., Stuefer, S. L. (n.d.). Hydrological and meteorological data from the North Slope of Alaska. Retrieved November 15, 2017, from http://ine.uaf.edu/werc/teon

Barry, R. G. (2017). The Arctic Cryosphere in the Twenty-First Century. In *Geographical Review*. https://doi.org/10.1111/gere.12227

Benson, C. S., & Sturm, M. (1993). Structure and wind transport of seasonal snow on the Arctic slope of Alaska. *Annals of Glaciology*, *18*(October), 261–267. https://doi.org/10.3189/S0260305500011629

Bintanja, R., & Selten, F. M. (2014). Future increases in Arctic precipitation linked to local evaporation and sea-ice retreat. *Nature*, *509*(7501), 479–482. https://doi.org/10.1038/nature13259

Bokhorst, S., Pedersen, S. H., Brucker, L., Anisimov, O., Bjerke, J. W., Brown, R. D., … Callaghan, T. V. (2016). Changing Arctic snow cover: A review of recent developments and assessment of future needs for observations, modelling, and impacts. *Ambio*, *45*(5), 516–537. https://doi.org/10.1007/s13280-016-0770-0

Callaghan, T. V, Johansson, M., Brown, R. D., Groisman, P. Y., Labba, N., Radionov, V., … Yang, D. (2011). The Changing Face of Arctic Snow Cover: A Synthesis of Observed and Projected Changes. *Ambio*, *40*, 17–31.

Deegan, L. A., Golden, H. E., Harvey, C. J., & Peterson, B. J. (1999). Influence of Environmental Variability on the Growth of Age-0 and Adult Arctic Grayling. *Transactions of the American Fisheries Society*, *128*(6), 1163–1175. https://doi.org/10.1577/1548-8659(1999)128<1163:IOEVOT>2.0.CO;2

Déry, S. J., & Wood, E. F. (2005). Decreasing river discharge in northern Canada. *Geophysical Research Letters*, *32*(10), 1–4. https://doi.org/10.1029/2005GL022845

Fatichi, S. (2009). Mann-kendall Test. Retrieved from https://www.mathworks.com/matlabcentral/fileexchange/25531-mann-kendall-test

Foster, J. L., Robinson, D. A., Hall, D. K., & Estilow, T. W. (2008). Spring snow melt timing and changes over Arctic lands. *Polar Geopgraphy*, *31*, 145–157. https://doi.org/10.1080/10889370802580185

Goodison, B., Louie, P. Y. T., & Yang, D. (1998). WMO solid precipitation measurement intercomparison. *Final Report*, (67), 318.

Hinzman, L. D. (1990). *The interdependence of the thermal and hydrologic properties of an arctic watershed and their response to climate change*. University of Alaska Fairbanks.

Hinzman, L. D., & Kane, D. L. (1991). Snow hydrology of a headwater Arctic basin 2. Conceptual Analysis and Computer Modeling. *Water Resources Research*, *27*(6), 1111–1121. https://doi.org/10.1029/91WR00262

Hinzman, L. D., Bettez, N. D., Bolton, W. R., Chapin, F. S., Dyurgerov, M. B., Fastie, C. L., … Yoshikawa, K. (2005). Evidence and Implications of Recent Climate Change in Northern Alaska and Other Arctic Regions. *Climatic Change*, *72*(3), 251–298.

https://doi.org/10.1007/s10584-005-5352-2
Hock, R. (2003). Temperature index melt modelling in mountain areas. *Journal of Hydrology*, *282*, 104–115. https://doi.org/10.1016/S0022-1694(03)00257-9
Holmes, R. M., Shiklomanov, A. I., Tank, S. E., McClelland, J. W., & Tretiakov, M. (2015). *River Discharge [in Arctic Report Card 2015]*. Retrieved from http://www.arctic.noaa.gov/Report-Card
Homan, J. W., Luce, C. H., McNamara, J. P., & Glenn, N. F. (2011). Improvement of distributed snowmelt energy balance modeling with MODIS-based NDSI-derived fractional snow-covered area data. *Hydrological Processes*, *25*(4), 650–660. https://doi.org/10.1002/hyp.7857
Kane, D. L., McNamara, J. P., Yang, D., Olsson, P. Q., Gieck, R. E., Kane, D. L., … Gieck, R. E. (2003). An Extreme Rainfall/Runoff Event in Arctic Alaska. *Journal of Hydrometeorology*, *4*(6), 1220–1228. https://doi.org/10.1175/1525-7541(2003)004<1220:AEREIA>2.0.CO;2
Kane, D. L., & Hinzman, L. D. (2017). Climate data from the North Slope Hydrology Research project. Retrieved November 15, 2017, from http://ine.uaf.edu/werc/projects/NorthSlope/coastal_plain/west_dock/west_dock.html
Kane, D. L., Gieck, R. E., & Hinzman, L. D. (1997). Snowmelt Modeling at Small Alaskan Arctic Watershed. *Journal of Hydrologic Engineering*, (2), 204–210.
Kane, D. L., Hinzman, L. D., Gieck, R. E., Mcnamara, J. P., Youcha, E. K., & Oatley, J. A. (2008). Contrasting extreme runoff events in areas of continuous permafrost, Arctic Alaska. *Hydrology Research*, *39*(4), 287–298. https://doi.org/10.2166/nh.2008.005
Kane, D. L., Youcha, E. K., Stuefer, S. L., Myerchin-Tape, G., Lamb, E., Homan, J. W., … Toniolo, H. (2014). *Hydrology and Meteorology of the Central Alaskan Arctic: Data Collection and Analysis Final Report*. Retrieved from http://ine.uaf.edu/werc/
Kane, D. L., Gieck, R. E., Kitover, D. C., Hinzman, L. D., Mcnamara, J. P., & Yang, & D. (2004). *Hydrological cycle on the North Slope of Alaska* (Vol. 290). IAHS Publ. Retrieved from http://hydrologie.org/redbooks/a290/iahs_290_0224.pdf
Kane, D. L., Gieck, R. E., Kitover, D. C., Hinzman, L. D., McNamara, J. P., & Yang, D. (2004). Hydrologic Cycles on the North Slope of Alaska. *Northern Research Basins Water Balance*, (December 2014), 224–236. https://doi.org/10.1017/CBO9781107415324.004
Kane, D., Youcha, E., Stuefer, S., Toniolo, H., Schnabel, W., Gieck, R., … Tape. (2012). *Meteorological and Hydrological Data and Analysis Report for Foothills/Umiat Corridor and Bullen Projects: 2006-2011*. Fairbanks, AK.
Katwijk, V. F., Rango, A., & Childress, A. E. (1993). Effect of Simulated Climate Change on Snowmelt Runoff Modeling in Selected Basins. *Journal of the American Water Resources Association*, *29*(5), 755–766. https://doi.org/10.1111/j.1752-1688.1993.tb03235.x
Larsen, J. N., Anisimov, O. A., Constable, A., A.B. Hollowed, N. Maynard, P. P., Prowse, T. D., & Stone, J. M. R. (2014). Polar Regions. *Climate Change 2014: Impacts, Adaptation, and Vulnerability. Part B: Regional Aspects. Contribution of Working Group II to the Fifth Assessment Report of the Intergovernmental Panel on Climate Change*, 1567–1612.
Lee, S., Klein, A. G., & Over, T. M. (2005). A comparison of MODIS and NOHRSC snow-cover products for simulating streamflow using the Snowmelt Runoff Model. *Hydrological Processes*. https://doi.org/10.1002/hyp.5810
Lilly, E. K., Kane, D. L., Hinzman, L. D., & Gieck, R. E. (1998). Annual water balacne for three nested watersheds on the North Slope of Alaska. In A. G. Lewkowicz & G. W. Kline (Eds.),

*7th International Permafrost Conference* (pp. 669–674). Retrieved from http://research.iarc.uaf.edu/NICOP/DVD/ICOP 1998 Permafrost 7th conf/CD-ROM/Proceedings/PDF001189/104189.pdf

Liston, G. E., & Hiemstra, C. A. (2011). The changing cryosphere: Pan-Arctic snow trends (1979-2009). *Journal of Climate*, *24*(21), 5691–5712. https://doi.org/10.1175/JCLI-D-11-00081.1

Mann, H. (1945). Mann Nonparametric test against trend. *Econometrica*, (13), 245–259.

Martinec, J. (1975). Snowmelt-Runoff Model for stream flow forecasts. *Nordic Hydrol.*, *6*(3), 145–154.

Martinec, J., & Rango, A. (1986). Parameter values for snowmelt runoff modelling. *Journal of Hydrology*, *84*(3–4), 197–219. https://doi.org/10.1016/0022-1694(86)90123-X

Martinec, Rango, & Roberts. (2008). *Snowmelt Runoff Model (SRM) User's Manual College of Agriculture and Home Economics*. Retrieved from http://aces.nmsu.edu/pubs/research/weather_climate/SRMSpecRep100.pdf

McNamara, J. P., Kane, D. L., & Hinzman, L. D. (1998). An analysis of streamflow hydrology in the Kuparuk River Basin, Arctic Alaska: a nested watershed approach. *Journal of Hydrology*, *206*, 39–57.

Meals, D. W., Spooner, J., Dressing, S. A., & Harcum, J. B. (2011). *Statistical Analysis for Monotonic Trends*. Fairfax, VA.

Mudryk, L., Brown, R., Derksen, C., Luojus, K., Decharme, B., & Helfrich, S. (2018). *Terrestrial Snow Cover [in Acrtic Report Card 2018]. State of the Climate in 2015*. Retrieved from http://www.arctic.noaa.gov/Report-Card

Nolan, M. (2002). Upper Kuparuk 5m DEM. Toolik Field Station GIS Portal.

Overland, J. E., Hanna, E., Hanssen-Bauer, I., Kim, S.-J., Walch, J. E., Wang, M., … Thomas, R. L. (2018). *Surface Air Temperature [in Arctic Report Card 2018]*. Retrieved from http://www.arctic.noaa.gov/Report-Card

Peterson, B. J., Holmes, R. M., Mcclelland, J. W., Vörösmarty, C. J., Lammers, R. B., Shiklomanov, A. I., … Rahmstorf, S. (2002). *Increasing River Discharge to the Arctic Ocean*. Retrieved from http://science.sciencemag.org/content/sci/298/5601/2171.full.pdf

Raleigh, M. S., Rittger, K., Moore, C. E., Henn, B., Lutz, J. A., & Lundquist, J. D. (2013). Ground-based testing of MODIS fractional snow cover in subalpine meadows and forests of the Sierra Nevada. https://doi.org/10.1016/j.rse.2012.09.016

Rittger, K., Painter, T. H., & Dozier, J. (2013). Assessment of methods for mapping snow cover from MODIS. *Advances in Water Resources*. https://doi.org/10.1016/j.advwatres.2012.03.002

Salas, J. D. (1993). Analysis and Modeling of Hydrologic Time Series. In D. R. Madiment (Ed.), *Handbook of Hydrology* (pp. 1–72). McGraw Hill Professional, 1993.

Schramm, I., Boike, J., Bolton, W. R., & Hinzman, L. D. (2007). Application of TopoFlow, a spatially distributed hydrological model, to the Imnavait Creek watershed, Alaska. *Journal of Geophysical Research: Biogeosciences*, *112*(G4), n/a-n/a. https://doi.org/10.1029/2006JG000326

Semmens, K. A., & Ramage, J. M. (2013). Recent changes in spring snowmelt timing in the Yukon River basin detected by passive microwave satellite data. *The Cryosphere*, *7*, 905–916. https://doi.org/10.5194/tc-7-905-2013

Steele, C., Dialesandro, J., James, D., Elias, E., Rango, A., & Bleiweiss, M. (2017). Evaluating MODIS snow products for modelling snowmelt runoff: Case study of the Rio Grande

headwaters. *International Journal of Applied Earth Observation and Geoinformation*, *63*, 234–243. https://doi.org/10.1016/J.JAG.2017.08.007

Stuefer, S., Kane, D., & Dean, K. (2019). *Snow water equivalent data from the Upper Kuparuk River watershed, Arctic Alaska, 1997-2017. Arctic Data Center*. Retrieved from doi:10.18739/A27M0405M.

Stuefer, S., Homan, J., Kane, D., Gieck, R., Youcha, E., & Hydrology Projects, U. (2014). *Snow Survey Results for the Central Alaskan Arctic, Arctic Circle to Arctic Ocean: Spring 2013*. Retrieved from http://ine.uaf.edu/werc/

Stuefer, S. L., Arp, C. D., Kane, D. L., & Liljedahl, A. K. (2017). Recent Extreme Runoff Observations From Coastal Arctic Watersheds in Alaska. *Water Resources Research*, 1–19. https://doi.org/10.1002/2017WR020567

Sturm, M., & Stuefer, S. (2013). Wind-blown flux rates derived from drifts at arctic snow fences. *Journal of Glaciology*. https://doi.org/10.3189/2013JoG12J110

Tekeli, A. E., Akyü Rek, Z., Arda Orman, A., Ensoy, A., & Nal Orman, A. (2005). Using MODIS snow cover maps in modeling snowmelt runoff process in the eastern part of Turkey. *Remote Sensing of Environme*, *97*(2), 216–230. https://doi.org/10.1016/j.rse.2005.03.013

Walker M. D., Walker D. A., & Everett K. R. (1989). Wetland Soils and Vegetation, Arctic Foothills, Alaska, (May). Retrieved from http://www.dtic.mil/dtic/tr/fulltext/u2/a323432.pdf

Woo, M.-K. (2010). Permafrost hydrology in North America Permafrost Hydrology in North America 1. https://doi.org/10.1080/07055900.1986.9649248

Yang, D., Goodison, B. E., Ishida, S., & Benson, C. S. (1998). Adjustment of daily precipitation data at 10 climate stations in Alaska: Application of World Meteorological Organization intercomparison results. *Water Resources Research*, *34*(2), 241–256. https://doi.org/10.1029/97WR02681

Youcha, E., Geick, R., & Kane, D. (2018). *Unpublished Upper Kuparuk Water Balance*. Fairbanks, AK.

# Appendix A

*Table A1. Summary of hydrometeorologic variables for the Upper Kuparuk.*

| Year | Peak Discharge cms | Date of Occurrence of Snowmelt Peak Julian Day | Volume Snowmelt Runoff mm | Cumulative Rainfall cm | SWE cm | May Positive Degree Days |
|---|---|---|---|---|---|---|
| **1993** | 13.9 | 140 | | | | |
| **1994** | 22.2 | 139 | | | | 71.5 |
| **1995** | 24.7 | 133 | | 298 | | 95.1 |
| **1996** | 26.2 | 150 | 77 | 221 | 14.7 | 71.4 |
| **1997** | 31.7 | 156 | 97 | 359 | 15 | 36.1 |
| **1998** | 9.6 | 145 | 38 | 219 | 8.1 | 116.1 |
| **1999** | 3.8 | 144 | 29 | 180 | 5.4 | 84.0 |
| **2000** | 32.6 | 158 | 78 | | 14.8 | 7.4 |
| **2001** | 15.8 | 154 | 74 | | 11.7 | 9.6 |
| **2002** | 21.6 | 144 | 41 | 256 | 10.5 | |
| **2003** | 41.3 | 157 | 113 | 147 | 13.9 | 12.3 |
| **2004** | 20.7 | 145 | 50 | 62 | 10.2 | 102.1 |
| **2005** | 10.5 | 134 | 54 | 145 | 10.9 | 88.3 |
| **2006** | 8.1 | 140 | 29 | 203 | 6.8 | 63.8 |
| **2007** | 16.1 | 147 | 39 | 100 | 10.2 | 40.4 |
| **2008** | 4.4 | 145 | 8 | 237 | 6.6 | 44.4 |
| **2009** | 28.4 | 144 | 50 | 243 | 13.1 | 42.5 |
| **2010** | 14.6 | 143 | 49 | 245 | 7.2 | 83.0 |
| **2011** | 50.0 | 143 | 92 | 117 | 11.3 | 99.8 |
| **2012** | 12.8 | 145 | 47 | 236 | 9.6 | 66.9 |
| **2013** | 37.4 | 154 | 67 | 233 | 11.3 | 8.6 |
| **2014** | 40.6 | 150 | 109 | | | |
| **2015** | 44.6 | 138 | 101 | 192 | 17.6 | 141.0 |
| **2016** | 16.2 | 134 | | 277 | 11.3 | 100.9 |
| **2017** | 12.7 | 144 | | 164 | 15.9 | 38.4 |

(Arp, C., Stuefer, 2017; D.L. Kane & Hinzman, 2017; Stuefer et al., 2019)

*Table A2. Summary of hydrometeorological variables for Imnavait Creek,AK*

| Year | Peak Discharge cms | Date of Occurrence of Snowmelt Peak Julian Date | Cumulative Rainfall cm | SWE cm | May Positive Degree Days |
|---|---|---|---|---|---|
| **1985** | 0.8 | 145 | | 10.6 | |
| **1986** | 0.6 | 156 | | 11.4 | |
| **1987** | 0.8 | 142 | | 10.2 | 69.3 |
| **1988** | 0.8 | 135 | | 7.5 | 80.3 |
| **1989** | 1.1 | 150 | | 12.6 | 48.4 |
| **1990** | 1.0 | 137 | | 9.9 | 167.4 |
| **1991** | 0.7 | 128 | | 8.2 | 55.1 |
| **1992** | 0.5 | 154 | | 15.3 | 26.2 |
| **1993** | 0.7 | 138 | | 10.1 | 92.1 |
| **1994** | 0.5 | 137 | | 8.0 | 65.7 |
| **1995** | 0.5 | 131 | 211 | 14.2 | 101.4 |
| **1996** | 1.2 | 146 | 148 | 10.2 | 72.6 |
| **1997** | 0.4 | 147 | 308 | 12.5 | 40.1 |
| **1998** | 1.1 | 154 | 246 | 9.5 | 96.0 |
| **1999** | 0.3 | 139 | 342 | 6.9 | 74.2 |
| **2000** | 1.1 | 156 | 232 | 11.2 | |
| **2001** | 0.8 | 153 | 204 | 12.7 | 19.2 |
| **2002** | 1.0 | 143 | 327 | 12.4 | 92.8 |
| **2003** | 0.7 | 154 | 325 | 15.7 | 13.9 |
| **2004** | 0.4 | 144 | 226 | 12.0 | 91.0 |
| **2005** | 0.6 | 133 | 56 | 11.9 | 98.9 |
| **2006** | 0.6 | 139 | | 9.6 | 96.4 |
| **2007** | 0.7 | 145 | 72 | 12.3 | |
| **2008** | 0.3 | 149 | 188 | 8.5 | 37.6 |
| **2009** | 0.5 | 144 | 360 | 17.4 | 54.3 |
| **2010** | | | 243 | | 111.8 |
| **2011** | | | 128 | | 113.7 |
| **2012** | 0.5 | 145 | 266 | 13.8 | 61.5 |
| **2013** | 2.0 | 149 | 259 | 19.3 | 31.5 |
| **2014** | 1.2 | 150 | | | 47.0 |
| **2015** | 1.6 | 136 | 206 | 19.8 | 144.1 |
| **2016** | 0.7 | 134 | 263 | 14.3 | 86.4 |
| **2017** | 0.8 | 139 | | 16.5 | 41.3 |

(Arp, C., Stuefer, 2017.; D.L. Kane & Hinzman, 2017)

*Table* A3. *USGS Summary data for Kuparuk River near Deadhorse, AK.*

| Year | Peak Discharge cms | Date of Occurrence of Snowmelt Peak Julian Date | Year | Peak Discharge cms | Date of Occurrence of Snowmelt Peak Julian Date |
|---|---|---|---|---|---|
| **1971** | 2180 | 156 | **1995** | 583 | 151 |
| **1972** | 1297 | 163 | **1996** | 1529 | 149 |
| **1973** | 2322 | 157 | **1997** | 1775 | 158 |
| **1974** | 680 | 161 | **1998** | 1464 | 149 |
| **1975** | 640 | 164 | **1999** | 634 | 155 |
| **1976** | 1557 | 167 | **2000** | 2495 | 165 |
| **1977** | 1892 | 157 | **2001** | 1557 | 161 |
| **1978** | 3341 | 158 | **2002** | 1416 | 144 |
| **1979** | 688 | 152 | **2003** | 1218 | 158 |
| **1980** | 1147 | 164 | **2004** | 850 | 155 |
| **1981** | 779 | 161 | **2005** | 988 | 160 |
| **1982** | 2945 | 158 | **2006** | 850 | 150 |
| **1983** | 1937 | 154 | **2007** | 1951 | 158 |
| **1984** | 1608 | 163 | **2008** | 850 | 152 |
| **1985** | 977 | 152 | **2009** | 1073 | 154 |
| **1986** | 1076 | 159 | **2010** | 1263 | 158 |
| **1987** | 439 | 155 | **2011** | 1608 | 151 |
| **1988** | 1096 | 164 | **2012** | 850 | 154 |
| **1989** | 2135 | 156 | **2013** | 2549 | 155 |
| **1990** | 1982 | 140 | **2014** | 1699 | 152 |
| **1991** | 1051 | 156 | **2015** | 2549 | 141 |
| **1992** | 736 | 153 | **2016** | 1427 | 145 |
| **1993** | 1481 | 154 | **2017** | 1138 | 152 |
| **1994** | 1034 | 159 | | | |

(Alaska Water Science Center; USGS; US Department of the Interior, 2017.)